Bull. Chem. Soc. Jpn., 71, 2509—2526 (1998)

Structural Genealogy of BEDT-TTF-Based Organic Conductors I. Parallel Molecules: β and β'' Phases

Takehiko Mori

Department of Organic and Polymeric Materials, Tokyo Institute of Technology, O-okayama, Tokyo 152-8552

(Received March 27, 1998)

A method is proposed to systematize a number of structural modifications of BEDT-TTF (bis(ethylenedithio)-tetrathiafulvalene)-based organic conductors and related materials. Analysis of actual crystal structures indicates that most crystal structures are constructed of two essential building blocks: "ring-over-bond" (RB) and "ring-over-atom" (RA) overlap modes. Several different ways to pile up these elements lead to various structures which are conventionally designated as β, β', β'', θ, α, and α''-phases. In the β- and β''-phases, introduction of "dislocations" along the stacking axis generates a number of modifications. Here dislocations mean interactions of two donor molecules which have larger displacements along the molecular long axis than the standard RB and RA modes. Systematic nomenclature to distinguish these modifications is proposed. Transfer integrals are, however, not very sensitive to the existence of dislocations, so that the Fermi surfaces of these multiple phases are derived from the fundamental structure by folding the first Brillouin zone.

Since the discovery of the first organic superconductor $(TMTSF)_2PF_6$ (TMTSF: tetramethyltetraselenafulvalene) in 1979,[1] a large variety of organic conductors have been synthesized; from these, more than 50 organic superconductors have been discovered.[2—4] Among them organic conductors based on BEDT-TTF (bis(ethylenedithio)tetrathiafulvalene or ET for short) form the largest and most important family. Nearly half of the organic superconductors so far found are radical-cation salts of ET, and the organic superconductor with the highest T_C to date (besides the fullerene compounds) is also based on the ET molecule; $\varkappa$-$(ET)_2Cu[N(CN)_2]Cl$ shows superconductivity at T_C = 12.8 K under a moderate pressure (0.3 kbar).[5]

It is characteristic of ET that this molecule forms a rich variety of phases with various anions. Up to now crystal structures of more than two hundred ET salts have been reported, among which only 24 show superconductivity. It is customary that the various crystal structures are classified as α, β, β', β'', θ, $\varkappa$, and so on. In the present paper we will show that these ET phases are derived from two kinds of overlap modes between two ET molecules. The ring-over-bond (RB) (sometimes called bond-over-ring) overlap mode has been well-known, but in ET salts is also important another overlap mode. We shall call this the "ring-over-atom" mode on the analogy of the ring-over-bond mode.

According to the various ways of piling up these elements, a large number of crystal structures, conventionally designated as α, β, β', β'', θ, and so on, are generated. These phase names are not systematic at all, owing to the complicated historic background. A history of the nomenclature is described in the Appendix.

In the β- and β''-phases, there are many modifications which are not strictly isostructural to each other but which do have a similar nearest-neighbor molecular arrangement. A method to systematize these modifications is proposed. A similar attempt has been undertaken earlier by Kistenmacher;[6] he has taken a unit of two ET molecules as the building block; by doubling this building block along the longitudinal and/or transverse directions, he has classified various structures of ET salts. He has, however, taken into account neither difference of overlap modes nor inclination. In the present paper we will attempt to classify all reported β- and β''-salts of ET, BO, and BETS (Scheme 1) (BO: bis(ethylenedioxy)tetrathiafulvalene, BETS: bis(ethylenedithio)tetraselenafulvalene). The classification given here is applicable to many other organic conductors as well. Detailed discussion of the θ-, α-, and $\varkappa$-phases, which have inclined molecules, will be given in a succeeding paper.[7]

It has been widely accepted that the Fermi surface of ET-based conductors can be predicted from a simple calculation where the transfer integrals are estimated from overlap of HOMO, and the band structure is calculated on the basis of the tight-binding approximation. Results of this kind of calculation agree well with such experiments as quantum oscillations and angle dependent magnetoresistance oscillations.[4] From this viewpoint, transfer integrals or equivalently overlap integrals of HOMO relate the arrangement of ET molecules in a crystal to the physical properties.

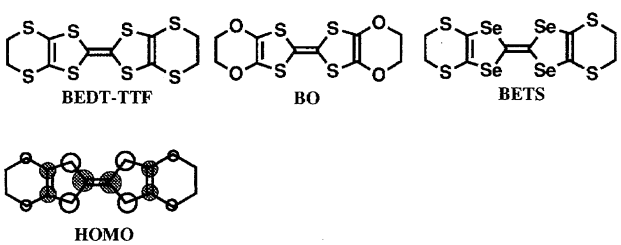

Scheme 1.

In 1984 we have investigated the change of overlap integrals systematically when the geometry of two ET molecules is changed.[8] In the present paper a similar calculation will be repeated so as to afford a quantum chemical background to the above classification of the crystal phases.

Overlap Modes of Parallel Molecules

Molecular Coordinates. In the beginning we shall examine how the transfer integral will change as the relative geometry of a pair of parallel ET molecules is modified. The details of the calculation methods are described at the end of this paper. First we shall define "molecular coordinates" as shown in Fig. 1(a), putting the origin of the *XYZ* axes on the center of a given ET molecule and making the *X* axis parallel to the molecular long axis, the *Y* axis parallel to the molecular short axis in the molecular plane, and the *Z* axis perpendicular to the molecular plane. From this definition, the *XYZ* coordinates of the center of another ET molecule represent the relative geometry of these ET molecules. The *X* coordinate, which is the displacement along the molecular long axis with respect to the given molecule, has been designated as *D* in Ref. 8. In addition, $\phi = \tan^{-1} Z/Y$ will sometimes be referred to as the angle between the molecular plane and the intermolecular vector.

Overlap Integrals in Parallel Molecules. The shape of HOMO is depicted in Scheme 1; HOMO of an ET molecule is a π-orbital where all sulfur pπ-orbitals have positive signs and all carbon pπ-orbitals are negative (shaded in Scheme 1). As shown in Fig. 1(b), the overlap integrals *S* of HOMO have been calculated when ϕ is changed from 0° to 90° by keeping the S–S contacts at 3.6 Å (Fig. 2(a)). Then, from 0° to about 47°, the second molecule is rotated around the line connecting the nearer sulfur atoms of the first molecule, and

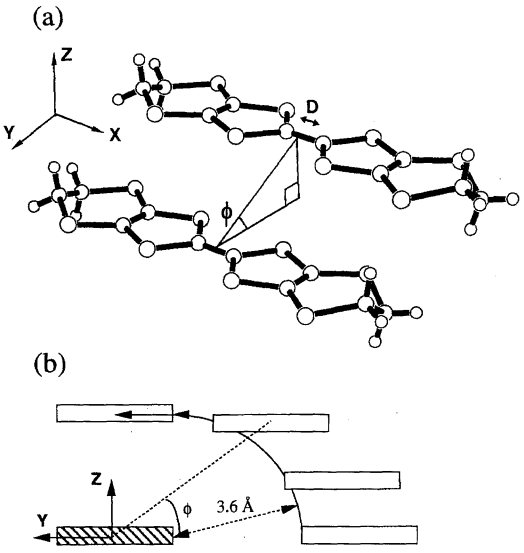

Fig. 1. (a) Definition of "molecular coordinates": *X* along the molecular long axis, *Y* along the molecular short axis in the molecular plane, *Z* perpendicular to the molecular plane, $D = \Delta X$, and $\tan \phi = Z/Y$. (b) Molecular movement in the calculation of Fig. 2(a).

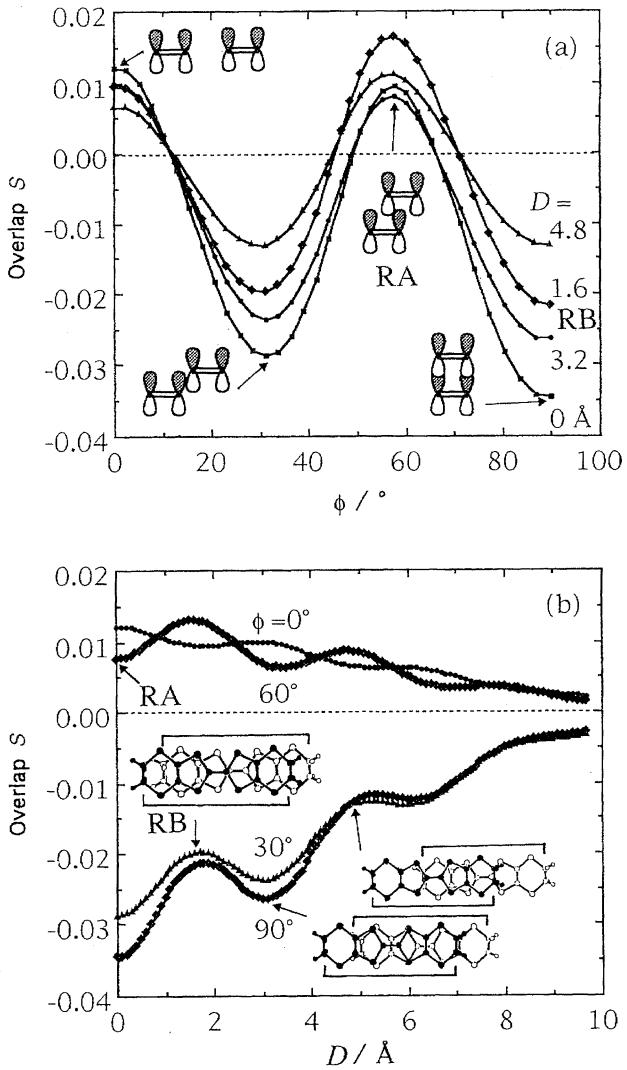

Fig. 2. (a) Overlap integrals between HOMO's of ET as a function of ϕ for several *D*. The molecules are moved as shown in Fig. 1(b). (b) Overlap integrals as a function of *D*. These values are calculated at $Y = 6.6$ Å, $Z = 0.0$ Å for $\phi = 0°$, $Y = 6.14$ Å, $Z = 1.70$ Å for $\phi = 30°$, $Y = 5.00$ Å, $Z = 2.88$ Å for $\phi = 60°$, and $Y = 0.0$ Å, $Z = 3.6$ Å for $\phi = 90°$.

from 47° to 90° the second molecule is moved approximately parallel to the *Y* axis.

As shown in Fig. 2(a), *the interaction makes maxima near $\phi = 0°$, 30°, 60°, and 90°*; the magnitude of the interaction does not depends on the *sign* of *S*, but depends only on its *absolute value*. Between these maxima *S* crosses zero near 12°, 40°, and 70°. In actual ET crystals, most geometries appear somewhere near these maximum angles, namely at $\phi = 0°$, 30°, 60°, and 90°. These geometries maximize bonding interaction between the ET molecules, but not only these electronic interaction but also the combination of the van der Waals interaction and other structural factors would be responsible for these packing patterns. Among them, the $\phi = 60°$ and 90° interactions are of special importance, because they determine the fundamental structural patterns of the molecular arrangement. It should be noted in Fig. 2(a)

that the peaks at $\phi = 0°$ and 60° are somewhat smaller than those at $\phi = 30°$ and 90°.

In Fig. 2(a) the calculations have been carried out for several D values. *The overlap integral S does not much depend on D*, because all sulfur π-orbitals have the same sign on the HOMO of the ET molecule (Scheme 1). This is also demonstrated in Fig. 2(b), where the D dependence of the overlap integral has been estimated for $\phi = 0°$, 30°, 60°, and 90°. In this calculation, Y and Z have been kept unchanged for each curve. The absolute value of the overlap integral $|S|$ is a slowly decreasing function of D, but the curves do not intercept zero at any D. As for $\phi = 0°$, 30°, and 90°, $|S|$ makes small maxima near $D = 0$ and 3.2 Å; these maxima correspond to the "eclipsed mode" of 1,3-dithiole rings (the five-membered rings of ET), where a 1,3-dithiole ring of one molecule comes just above the 1,3-dithiole ring of another molecule. Since the length of a 1,3-dithiole ring (or equivalently the S–S distance along the molecular long axis in a molecule) is about 3.2 Å, $|S|$ weakly undulates with this periodicity. In the middle of these maxima, namely at about $D = 1.6$ and 4.8 Å, the overlap makes minima. In these configurations, a sulfur atom of a given molecule comes to the middle of the two sulfur atoms of another molecule.

Ring-Over-Bond Overlap Mode. The 90° interaction makes the ordinary face-to-face stacking. In particular, the $\phi = 90°$ and $D = 1.6$ Å configuration is known as ring-over-bond-type overlap (hereafter abbreviated as RB mode for short). This configuration is shown in Fig. 3(a). In the calculation, this corresponds to a *minimum* of $|S|$ because the interplanar spacing Z has been artificially kept constant, but in an actual crystal this realizes closest S–S contacts and shortest interplanar spacing, leading to the optimal overlap.[9]

Ring-Over-Atom Overlap Mode. The 60° interaction is obviously different from this ordinary stacking. To distinguish this mode from the ordinary face-to-face stacking, we shall call this mode "pseudo-stacking." Although this pseudo-stacking is not very familiar in conventional quasi-one-dimensional organic conductors, it appears as frequently as the ordinary stacking in ET-based organic conductors.

When $\phi = 60°$, as shown in Fig. 2(b), the positions of the maxima and minima are inverted; instead of maxima, *minima* of $|S|$ appear at $D = 0$ and 3.2 Å. The minimum at $D = 0$ Å corresponds to the configuration in Fig. 3(b), where a sulfur atom comes above the center of the 1,3-dithiole ring of another molecule. This configuration again avoids steric S–S repulsion and realizes optimal S–S contacts. In contrast to the RB mode, we shall call this geometry "ring-over-atom" (RA) overlap mode.

To further demonstrate that this configuration brings about an optimal overlap, we have calculated the overlap when the second molecule is moved horizontally (Fig. 4) (namely by changing Y with keeping X and Z constant). Starting from the maximum at $Y = 0$ Å (this corresponds to the ordinary face-to-face stacking), the overlap crosses zero at around $Y = 1.5$ Å, and attains a maximum near $Y = 2$ Å; this geometry corresponds to $\phi = 60°$ (see the upper scale of Fig. 4). Since the width of an ET molecule (the S–S distance along the molecular short axis in a molecule) is about 3.2 Å, $Y = 2$ Å corresponds to half and a little of the ring width, so a sulfur atom comes above the 1,3-dithiole ring of another molecule (Fig. 3(b)). This behavior of the overlap integral emerges from the symmetry of HOMO; all sulfur atoms have plus signs and all carbons have minus signs. At $Y = 0$ Å, π-orbitals of S–S (and C–C) atoms overlap in phase, near $Y = 2$ Å π-orbitals of S and C atoms overlap, and near $Y = 4$ Å π-orbitals of S–S atoms which are located at the opposite sides of each molecule give rise to another maximum.

When we investigate the geometry of ET molecules observed in actual crystals by picking up every pair of ET molecules, as will be exemplified in the following sections, we find that most frequently the RB and RA overlap modes are realized. Interactions with larger D appear on some occasions, but very seldom "eclipsed" configurations appear such as the interaction at $\phi = 90°$ and $D = 0$ Å. D dependence of overlap is small, but the existence of large-D interaction is

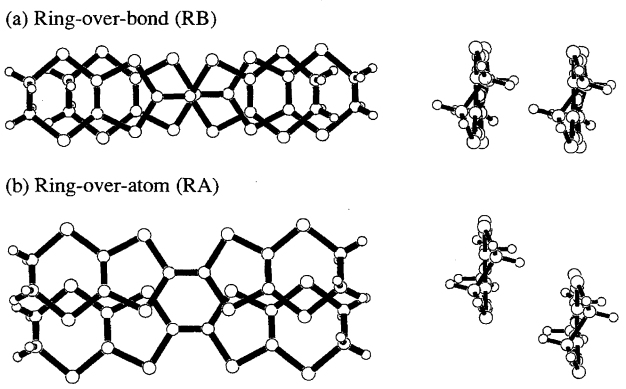

Fig. 3. (a) "Ring-over-bond (RB)" and (b) "ring-over-atom (RA)" overlap modes viewed perpendicular to the molecular plane (left) and along the molecular long axis (right).

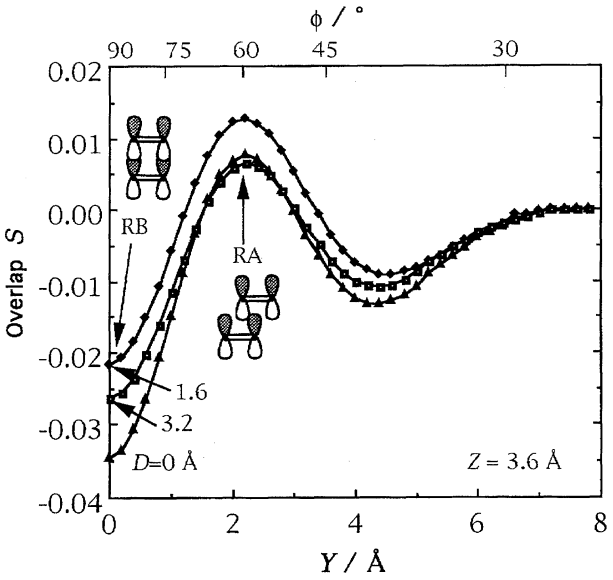

Fig. 4. Overlap integrals as a function of Y at $Z = 3.6$ Å, for several D values. The upper scale represents are corresponding ϕ values.

important in determining the packing pattern of the donors. In the beginning, we shall show that, by neglecting the difference of D, we can construct a variety of phases by piling up the RB and RA modes.

Genealogy. As shown in Fig. 5, when the RB mode is repeated in one direction, the usual "face-to-face" stack is constructed. This pattern has been called β-phase in ET salts.

When the RA mode is repeated, a pseudo-stack, which is made up of inclined molecules, is formed. The structure constructed of the RA mode gives a few modifications depending on the direction of the inclination. The structure where all stacks have the same (parallel) inclination has been called β''-phase.

If the slopes are alternately oriented in the opposite directions in the adjacent stacks, θ-phase is generated. When the θ-phase is weakly dimerized along the stacking direction, α-phase is produced. It is also possible that two types of inclination appear like $++--++--++--\cdots$ (+ and − represent downward and upward slopes, respectively). This phase has sometimes been called α''-phase. In this phase, the two parallel chains form a structure similar to the β''-phase; then α''-phase is regarded as a 1 : 1 hybrid of θ- and β''-phases. From the viewpoint of the relation to other phases, $\varkappa$-phase takes an exceptional position and is unable to be discussed in this context; the relation of $\varkappa$-phase to θ-phase will be discussed in the succeeding paper.[7]

Since the differences of β, β'', and θ-phases are characterized by the inclination, we can imagine that, as shown in Fig. 6, these phases are related to each other by the hypothetical rotation of the molecular planes. When the molecular planes of the θ-phase are rotated alternately in the opposite directions so as to make all molecules parallel to each other, β-phase is produced (Fig. 6(a)). On the other hand, the β''-phase is obtained by rotating the molecules of every other column of the θ-phase, if we keep the other columns unchanged so as to make all molecular planes parallel again (Fig. 6(b)).

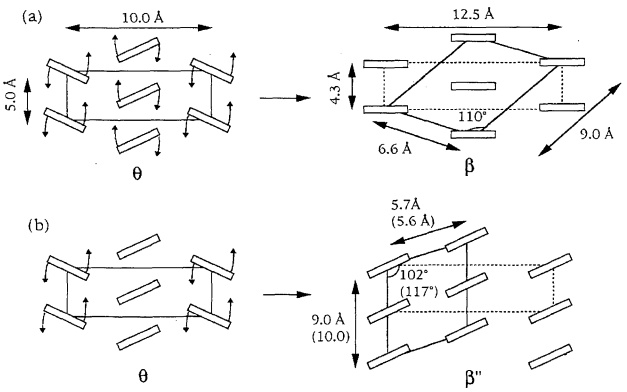

Fig. 6. β and β''-phases generated by hypothetical molecular rotation from the θ-phase. The lattice constants are shown. The values in the parentheses in the β''-phase are estimated from those of the θ-phase.

Although these operations are entirely artificial, we can estimate the size of the unit cells from these relations. In the θ-phase, the lattice constant along the stacking direction is typically 5 Å, and the transverse lattice constant is about 10 Å. In an actual β-phase, the unit cell is a parallelogram as shown in Fig. 6(a), owing to the introduction of "dislocations" (vide infra). After a little calculation we can estimate the corresponding lengths of the stacking and transverse directions, as shown in Fig. 6(a). On account of the rotation, the cell expands in the transverse direction (10 to 12.5 Å), but somewhat shrinks in the stacking direction (5 to 4.3 Å). From this we can understand that in the θ-phase the ratio of the lattice constants in the stacking and transverse directions is closely related to the inclination angle of the molecular planes. This gives an important clue to explain the universal phase diagram of the θ-phase.[7]

On the other hand, in the β''-phase, the unit cell changes to a parallelogram again, as shown in Fig. 6(b). When we estimate the lattice constants of the β''-phase from the θ-phase, the results are not largely different from the real lattice constants (5.6 Å for the real 5.7 Å and 10.0 Å for 9.0 Å).

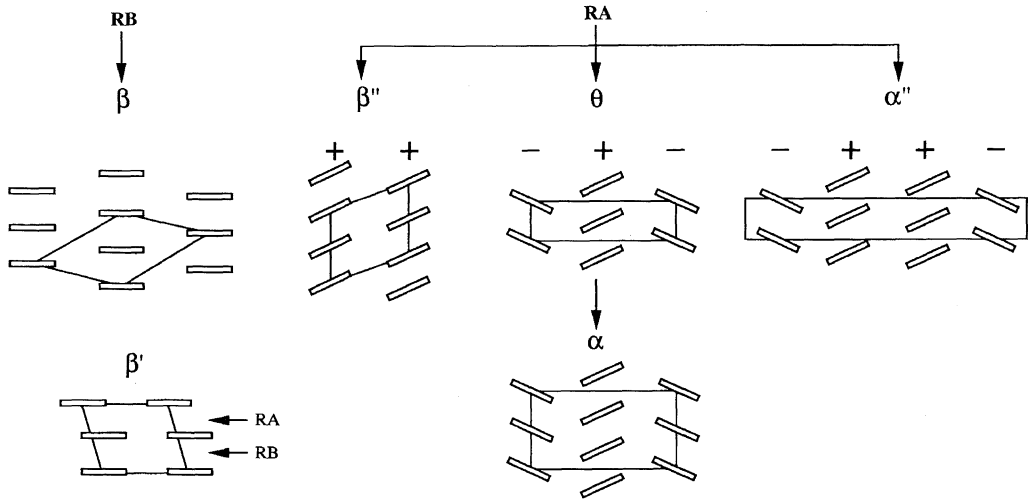

Fig. 5. Genealogy of β, β', β'', θ, α, and α''-phases; the packing patterns of the donor sheets are viewed along the molecular long axis.

This relation enables a kind of disorder where the inclination of every other stack is a random mixture of two possibilities (upward and downward) in a crystal, and the structure is a hybrid of the β''-phase and the θ-phase. Such a disorder has been recently reported in $(ET)_2[C(SO_2CF_3)_3]$.[10]

Modifications of β-Phase Salts

A chain of β-phase crystal is composed of a stack of the RB mode (Fig. 5). The calculation of overlap integral has showed that D = 1.6 Å is preferable in the ordinary $\phi = 90°$ stacking (RB mode). However, the non-planarity of the ET molecule and the accordance with the anion size require the existence of large-D overlaps, which we shall call "dislocation." In the actual β-phases, various combinations of the ordinary RB mode and dislocations give rise to many modifications of the β-phase.

Variations of Stacking Structures. There are two ways in piling up a simple stack of the RB mode; D may be chosen alternately in the opposite directions like +− +− (Fig. 7(a)), or chosen in the same direction like ++++ (Fig. 7(b)). The former is seen in $(TMTSF)_2X$,[11] so we shall designate this structure as $(TMTSF)_2X$ type. The latter constructs the widely observed regular stack; a well-known example is the TTF stack in (TTF)(TCNQ) (TTF: tetrathiafulvalene, and TCNQ: tetracyanoquinodimethane).[12]

In Fig. 8(a) the donor sheet structure of $(TMTSF)_2X$ is depicted, together with D values for each interaction. Both kinds of stacking modes, a1 and a2, are the ordinary RB overlap mode; the D values are 1.6 Å and −1.5 Å, respectively. The b interaction has unusually large D (3.2 Å); this corresponds to one unit of a 1,3-dithiole ring. Since the b interaction connects the equivalent molecules in the neighboring chains, this D value means that the adjacent chains are displaced by D = 3.2 Å. Consequently, D of the p2 interaction is very large, 4.6 Å. Such large transverse displacements are not observed in ET-based conductors, and this is partly responsible for the comparatively strong one-dimensional nature of this compound.

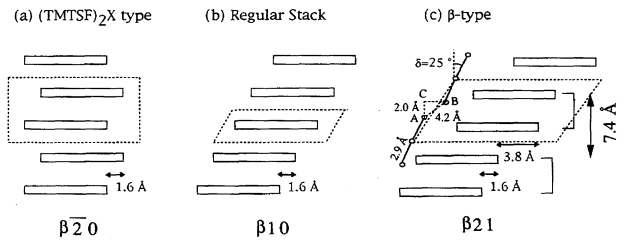

Fig. 7. Stacking patterns of (a) $(TMTSF)_2X$, (b) regular chain in (TTF)(TCNQ), and (c) the β-phase, viewed along the molecular short axis.

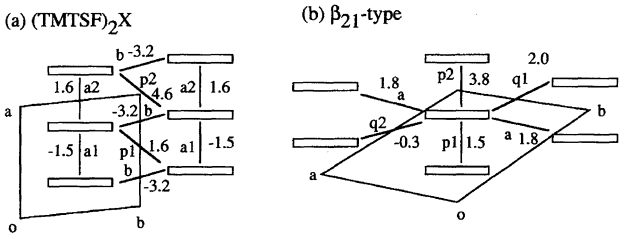

Fig. 8. Structure of donor sheets, and the D values in (a) $(TMTSF)_2X$ and (b) β-$(ET)_2I_3$, viewed along the molecular long axis.

Neither (TMTSF)$_2X$ type nor (TTF)(TCNQ) type regular stacks have been observed in ET salts. This is because of the steric hindrance of the ET molecule. It is well known that the ethylene groups of the ET molecule are out of the molecular plane, which therefore prevent the regular stacking of the molecules. This is an important reason that ET forms two-dimensional conductors rather than one-dimensional ones. In the $(TMTSF)_2X$ type structure, one end of a molecule is sandwiched between two adjacent molecules (Fig. 7(a)) by inhibiting the terminal atoms from going out of the molecular plane. Thus the ethylene part of an ET molecule is unable to come to this position.

In the case of (TTF)(TCNQ) type regular stack (Fig. 7(b)), at all times one side of a molecular terminal is open. This structure is not found in ET salts either. The two ethylene parts of an ET molecule are chemically equivalent to each other. However, in actual crystals, one ethylene group is significantly out of the molecular plane, while another ethylene group is only slightly deviated from the molecular plane. Probably the regular stack does not provide sufficient space to incorporate this largely deviated ethylene part.

In order to make the sufficient open space for the deviated ethylene, an ET column in general has larger D (dislocation) for every other molecule (Fig. 7(c)). This is the β-type structure observed in β-$(ET)_2I_3$. In Fig. 8(b), the donor sheet structure of β-$(ET)_2I_3$ is depicted, and the parameters which represent the geometry of interactions (molecular coordinates and ϕ) are listed in Table 1. The value of interdimer D (for the p2 interaction) is about 3.8 Å; this is in between the length of one 1,3-dithiole ring, 3.2 Å, and the length of one and a half rings 4.8 Å. The former corresponds to an eclipsed mode but the latter to another ring-over-bond overlap. The actual geometry comes in the middle of these modes, suggesting that the magnitude of D is not decided by the optimal overlap nor other electronic reason, but rather comes from structural factors, e.g. the anion length as discussed below. Then the stack in the β-phase suffers from fairly strong dimerization, which is represented by the significant difference of p1 and p2 overlap integrals (Table 1), resulting in two-dimensional Fermi surfaces.[13]

As for the transverse interactions of the β-phase (see Ta-

Table 1. Overlap Integrals ($\times 10^{-3}$) and Geometry Parameters in β-$(ET)_2I_3$

Interaction	Overlap	X (D) /Å	Y /Å	Z /Å	ϕ /°
p1	−24.5	1.5	0.1	3.6	87
p2	−8.4	3.8	0.4	3.9	84
q1	−12.7	2.0	5.7	2.4	22
q2	−6.8	0.3	6.3	2.1	18
a	−5.0	1.8	6.1	1.5	14

For the definition of interactions, see Fig. 8(b). The coordinates, X, Y, Z, and ϕ are defined in Fig. 1.

ble 1), the basic slide distance between adjacent chains does not much exceed 1.6 Å; D for the q1, q2, and c interactions are 2.0, 0.3, and 1.8 Å, respectively (Fig. 8(b)). Despite the large D in p2, there appear no large D along the transverse directions.

The transverse ϕ values are between 14° and 22° (Table 1). In the plot of ϕ dependence of S (Fig. 2(a)), these values correspond to the tail of the 30° peak, but are not close to the maximum. This suggests that the transverse interaction of the β-phase is not determined by purely electronic reason, but probably prescribed by the structural factor.

Anion Length and Dislocation. There is another reason for the significantly strong dimerization in the β-phase. Since the sum of the interplanar distance in a unit cell is 7.4 Å, if the molecular planes are exactly perpendicular to the stacking axis as in Fig. 7(a), the repeating unit along the stack should be 7.4 Å. However, an I_3^- anion is 9.6 Å in length. Because the lattice constant in the transverse direction is much smaller (6 Å), linear anions are usually located parallel to the stacking axis.

There is a rule generally observed in many crystals; *in a salt of a linear anion, the direction of the anion corresponds to the intermolecular vector between the centers of stacked molecules*. In the case of regular stacks, this direction is the same as the stacking direction. In the case of dimerized (or trimerized) stacks, the anion direction is parallel to the intermolecular vector between the centers of the dimerized (or trimerized) molecules. This rule is probably based upon the structural requirement that the linear anion has to be incorporated parallel to the "edge line" of the dimer. In the dimerized or trimerized structures, the anion direction is therefore slightly inclined with respect to the stacking direction.

From this view it is impossible that an I_3^- anion is incorporated in the stack of Fig. 7(a). In the case of a regular stack shown in Fig. 7(b), the unit cell length L is to be 8.0 Å, and this L is still too short. From the discussion of the preceding paragraph, the I–I direction (designated as 2.9 Å in Fig. 7(c)) is always inclined by 25° from the vertical direction, because the inclination of a dimer is always the same as that of a regular stack (see Chapter "Inclination from the Stacking Direction"). For the regular stack, the vector AB in Fig. 7(c) is also parallel to the lattice, and the distance AC is estimated to be (8.0 Å—2×2.9 Å)cos 25° = 2.0 Å. When we increase the interdimer displacement D, we may move the dimer unit horizontally, together with an I_3^- anion located at the same level as the dimer. At the same time BC increases, but AC is unchanged as far as the intermolecular spacings are unchanged. In order to make the inter-anion I–I distance (AB) larger than the van der Waals distance of I^-, 4.2 Å, the distance BC has to exceed 3.75 Å. This BC distance is directly equal to the interdimer displacement D, and also approximately equal to the actually observed D = 3.8 Å of the p2 interaction (Table 1). This calculation demonstrates that D = 3.8 Å for p2 is determined from the size of the I_3^- anion. In the case of IBr_2^- and AuI_2^- (I–Br: 2.702 Å and Au–I: 2.56 Å), the same calculation gives D = 3.5 and 3.3 Å, respectively. In the actual IBr_2^- salt, D shrinks to 3.6 Å.

Systematic Nomenclature of Various β-Phases. The interdimer interaction p2 with large D = 3.8 Å is regarded as a "dislocation" introduced in the stack. Here we shall define *a "dislocation" as an interaction with D significantly larger than 1.6 Å of the standard RB overlap mode.*

There are possibilities of more complicated structures where the dislocation appears every three or four molecules, constructing trimerized or tetramerized structures. To distinguish these modifications we shall introduce a systematic nomenclature. We have to specify two numbers, one of which represent the periodicity along the stacking axis, and another of which is the number of the dislocations within the repeating unit. By making these numbers subscripts, the ordinary β-phase is designated as β_{21}, in which *the first subscript 2 stands for the periodicity and the second subscript 1 represents the number of dislocations within the repeating unit.* By this definition, the regular stack shown in Fig. 7(b) will be represented as β_{10}. $(TMTSF)_2X$ structure will be designated as $\beta_{\bar{2}0}$, where $\bar{2}0$ means that the displacements occur alternately in the opposite directions.

Multiple β-structures are classified according to this notation. ET and BETS-based β-phases are listed in Table 2. For example, from notation like β_{11}-(ET)$CuCl_2$ we can understand that each donor molecule in this phase is almost isolated from others. The ordinary β_{21}-phases are superconductors except for β_{21}-$(ET)_2I_2Br$, where the orientational disorder of the asymmetric I–I–Br anion has been believed to destroy the superconductivity. It is well known that in these β_{21}-phases the superconducting transition temperature decreases with decreasing the lattice volume (in the order of Table 2).[3] $\beta_{\bar{2}1}$-$(ET)_2AuCl_4$ is different from the ordinary β_{21}-phase, because D values of this phase change sign like 1.60 Å and −3.44 Å, so that intra- and inter-dimer displacements take place in the opposite directions.

$\beta_{21\times2}$-$(ET)_2ReO_4$ and the isostructural BrO_4 salt are named like this because along the transverse direction a unit cell contains two β_{21}-chains. Therefore a unit cell involves 2×2 = 4 donor molecules. These $\beta_{21\times2}$-salts undergo metal insulator transitions. Below the transition temperature of $\beta_{21\times2}$-$(ET)_2ReO_4$, as abrupt drop of spin susceptibility accompanied by the sharp decrease of ESR linewidth has been observed.[38] This transition is suppressed under pressure, and a superconducting phase appears at 2 K under 4 kbar.[39]

The β_{41}-phase is a structure made up of tetramers which are divided by one dislocation. This structure has not been found in ET-based salts, while it has been observed in β_{41}-$(CPTM\text{-}TTP)_4PF_6$ (CPTM-TTP: 2-(4,5-cyclopenteno-1,3-dithiol-2-ylidene)-5-(4,5-bis(methylthio)-1,3-dithiol-2-ylidene)-1,3,4,6-tetrathiapentalene).[40] By contrast, in the β_{42}-phase two dimers construct a repeating unit. In other words, four molecules build up the repeating unit, and two dislocations are involved within it. This phase is distinguished from the β_{21}-phase because of the difference of the two interdimer interactions. This structure has been realized in β_{42}-$(ET)_2InBr_4$.

Table 2. Lattice Parameters of β-Phase ET and BETS Salts

Pattern	Compounds	a /Å	b /Å	c /Å	γ /°	V /Å^3	T_{MI}	Ref.
β-phase								
11	(ET)$CuCl_2$	5.781	6.577	12.154	94.74	425.1	Insulator	14
21	$(ET)_2I_3$	6.597	9.070	15.243	109.73	848.9	T_{SC} = 1.5 K	13
	$(ET)_2AuI_2$	6.603	9.015	15.403	110.66	845.2	T_{SC} = 3.8 K	15
	$(ET)_2I_2Br$	6.612	9.024	15.192	110.12	842.3	Metal	16
	$(ET)_2IBr_2$	6.593	8.975	15.093	110.54	828.7	T_{SC} = 2.5 K	17
$\bar{2}1$[a]	$(ET)_2AuCl_4$	6.590	8.561	18.319	119.47	845.1	?	18
21[b]	α-$(ET)_2PF_6$	6.462	8.597	14.711	95.71	794.3	Insulator	19
21 × 2[c]	$(ET)_2BrO_4$	7.795	12.613	17.148	88.74	1589	150 K	20
	$(ET)_2ReO_4$	7.798	12.579	17.102	88.97	1584	81 K(SC)[d]	20
21 × 2[e]	$(ET)_4Cu(C_2O_4)_2$	8.684	11.776	15.832	93.69	1560	65 K	21
33[e]	$(ET)_3Cl$(*p*BIB)[f]	9.258	10.184	15.578	106.87	1358	Metal	22
	$(ET)_3Br$(*p*BIB)[f]	9.418	10.187	15.420	106.89	1372	Metal	22
42	$(ET)_2InBr_4$	6.681	17.470	16.040	92.43	1820	Insulator	23, 24
42 × 2[c]	$(ET)_2Fe(C_{12}H_{26}B_{18}S_2)$	11.638	17.717	25.748	90.0	5289	Insulator	25
75	$(ET)_5Hg_3Br_{11}$	12.977	14.454	26.404	92.44	4585	120 K	26
10,?	$(ET)_5[CuHg(SCN)_4]_2$	13.020	20.497	36.353	90.0	9651	180 K	27
11,5?	$(ET)_{11}[P_2W_{18}O_{62}](H_2O)_3$	14.597	18.418	42.271	107.82	10819	220 K	28
12,6[b]	$(ET)_3Li_{0.5}Hg(SCN)_4(H_2O)_2$	15.583	19.721	36.395	90.0	11181	170 K	29
β'-phase								
	$(ET)_2AuCl_2$	6.640	9.763	12.766	99.47	802.0	Insulator	30
	$(ET)_2ICl_2$	6.645	9.771	12.921	98.63	814.3	Insulator	31
	$(ET)_2IClBr$	6.642	9.816	12.975	98.28	821.3	Insulator	32
	$(ET)_2Cr(C_4H_{22}B_{18})$	6.634	7.995	21.944	76.52	1121.7	Insulator	25
	(ET)(TCNQ)	6.650	7.817	23.915	94.33	1197.0	310 K	33
	$(ET)_3(ZnCl_4)_2$	6.80	9.64	20.39	101.4	1307	Insulator	34
	$(ET)_3(MnCl_4)_2$	6.802	9.714	20.595	101.66	1329.8	Insulator	35
BETS salts								
42	λ-$(BETS)_2GaCl_4$	6.595	16.156	18.934	96.76	1776.3	T_{SC} = 8 K	36
	λ-$(BETS)_2FeCl_4$	6.593	16.164	18.538	96.76	1773.0	T_{MI} = 8 K	37

a) D of this $\beta_{\bar{2}1}$-phase changes sign like 1.60 Å and −3.44 Å so that intra- and inter-dimer displacements take place in the opposite directions, whereas the ordinary β_{21}-phase have the same sign of D. b) In these salts, intradimer overlap is eclipsed (D = 0 Å), and interdimer overlap is slid by D = 3.0—3.9 Å. c) ×2: Two-fold periodicity in the transverse direction. d) Superconductivity under pressure. e) The stack is inclined along the molecular short axis, so that the intrastack ϕ values are around 78°. f) *p*BIB: *p*-bis(iodoethynyl)benzene.

Although the ET-based β_{42}-phase is a poor conductor, the BETS-based β_{42}-phases are good conductors; λ-$(BETS)_2GaCl_4$ is a superconductor (T_{SC} = 8 K),[36] and λ-$(BETS)_2FeCl_4$ undergoes a characteristic metal-insulator transition at 8 K.[37] The λ-phase is represented as β_{42}-phase in the systematic nomenclature. The systematic nomenclature clarifies the relation of this structure to other β-phase compounds.

In α-$(ET)_2PF_6$ (in spite of such naming, this salt has β_{21}-structure) and $\beta_{12,6}$-$(ET)_3Li_{0.5}Hg(SCN)_4(H_2O)_2$, eclipsed dimers ($\phi$ = 90° and D = 0 Å) are realized instead of the usual RB overlap. In the latter compound, six dimers form the repeating unit.[29] Surprisingly, this complicated salt shows metallic conductivity down to 170 K. There are a few other compounds that have more than ten-fold periodicities (Table 2). In the β-phase ET salts which undergo metal-insulator transitions, as far as we know, in general the magnetic susceptibility drops below the transition temperature.

Fermi Surface of β-Phases. The magnitude of the overlap integral is not very sensitive to the value of D, as shown in Fig. 2(b). Accordingly, the Fermi surface of the multiple phases like β_{41} and β_{42} are, as a zeroth approximation, basically similar to that of the ordinary β_{21}-phase. The Fermi surface of the ordinary β_{21}-$(ET)_2I_3$ is depicted in Fig. 9(a); it consists of a cylinder whose cross section is half of the first Brillouin zone in the conducting plane.[13] The repeating unit of the β_{42}-phase in the stacking direction is twice as large as that of the β_{21}-phase, so that the Brillouin zone is folded by half. If the Fermi surface is unchanged, it crosses the zone boundary because its cross section is equal to the first Brillouin zone (Fig. 9(b)). This situation is the same as the $\varkappa$-phase.[41] On account of the lower symmetry, in an actual λ-phase, the degeneracy on the zone boundary is removed, then the Fermi surface is separated into a closed part and an open part. This picture agrees well with the reported Fermi surface of the λ-phase.[36,37] This argument is similar to the transformation from the θ-phase to the α-phase (Fig. 10(c) and Fig. 10(d)).[7] The situation of β_{41}-(CPTM-TTP)$_4PF_6$ is similar to Fig. 9(b), but the band filling is half owing to the 4 : 1 composition, and the cross section of the Fermi surface is half. Hence the Fermi surface does not cross the zone boundary; the surface has an elliptical cross section,

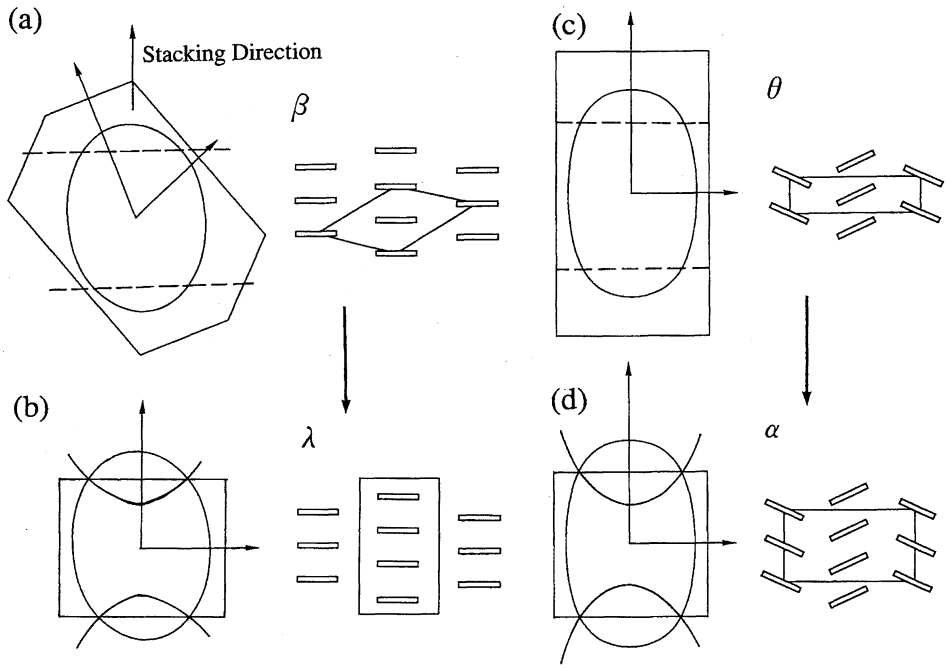

Fig. 9. Fermi surface of (a) β- and (b) λ-phases. Folding the Fermi surface of β_{21}-phase generates that of λ (= β_{42})-phase, in analogy with α-phase (d) made from θ-phase (c).[85]

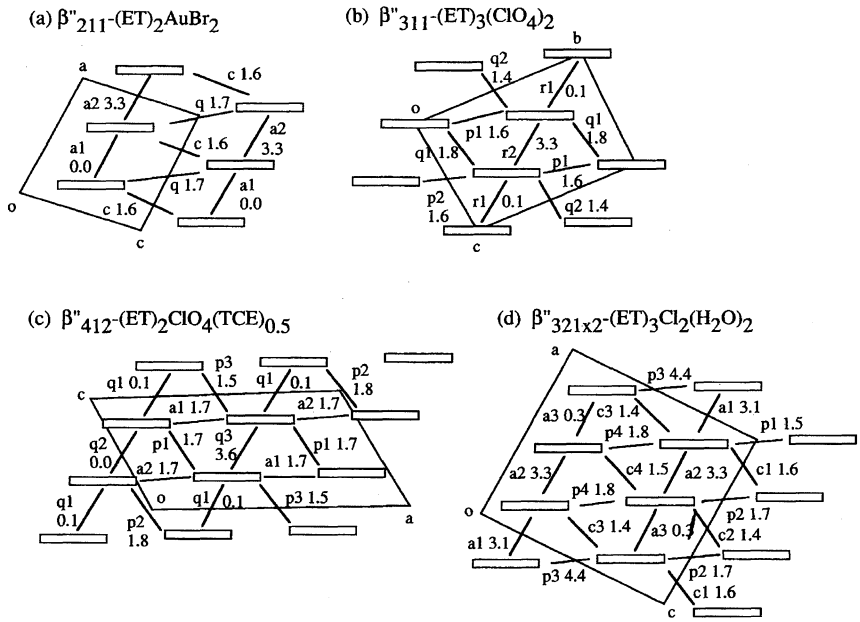

Fig. 10. Structure of donor sheets, and the D values in (a) β''_{211}-$(ET)_2AuBr_2$, (b) β''_{311}-$(ET)_3(ClO_4)_2$, (c) β''_{412}-$(ET)_2ClO_4(TCE)_{0.5}$, and (d) $\beta''_{321\times2}$-$(ET)_2Cl_3(H_2O)_2$, viewed along the molecular long axis.

and looks like Fig. 9(a).[41]

Modifications of β''-Phase Salts

Two-Fold Structures. The β''-phase does not contain a usual "face-to-face" stack of ϕ = 90°, but consists of the pseudo-stack of the RA overlap mode (Fig. 5). This "stacking" direction corresponds to ϕ = 60°, and other transverse interactions extend in the ϕ = 30° and 0° directions. Then the β''-phase has a network of 0°–30°–60° interactions. If we neglect the anisotropic shape of the ET molecules, this network looks like a "hexagonal" lattice.

The β''-phase in a narrow sense is not a very common phase; it appears only in β''-$(ET)_2AuBr_2$ and a few isostructural salts (Table 3).[42] The donor sheet structure of β''-$(ET)_2AuBr_2$ is depicted in Fig. 10(a). In the pseudo-stacking direction, D is alternatively 0.0 Å (a1) and 3.3 Å (a2). It is noteworthy that this displacement D = 3.3 Å corresponds to the length of a 1,3-dithiole ring. In the ϕ = 60° interaction, D = 0 Å realizes the "ring-over-atom" configuration, where a sulfur atom comes on the top of the 1,3-dithiole ring, making the overlap optimal (Fig. 3(b)). Besides D = 0 Å, the D = 3.3 Å interaction is another optimal overlap. Because the D = 0

Table 3. Lattice Parameters of β''-Phase ET and BO Salts

Pattern	Compounds	a /Å	b /Å	c /Å	γ /°	N[a]	T_{MI}	Ref.
20	$(ET)_2Cl(DIA)$[b]	6.728	7.642	17.477	106.90	2	Metal	22
210	$(ET)_2[N(SO_2CF_3)_2]$	6.639	8.658	17.349	68.95	2	?	43
211	$(ET)_2AuBr_2$	5.712	9.027	16.372	102.94	2	Metal	42
	$(ET)_2ICl_2$	5.769	9.003	16.290	103.64	2	Metal	44
	$(ET)_2AuBrI$	5.770	9.071	16.406	103.43	2	Metal	45
	$(ET)_2Cl_2SeCN$	5.924	8.722	16.249	92.688	2	200 K	46
	$(ET)_2Br_2SeCN$	5.930	8.804	16.509	92.192	2	200 K	46
211×2[c]	$(ET)_2SF_5CF_2SO_3$	11.440	9.154	17.491	102.76	4	$T_{SC}=5.2$ K	47
$211+210\times2$	$(ET)_2CuCl_4H_2O$	16.634	8.980	16.225	93.24	6	Metal	48
311	$(ET)_3(FSO_3)_2$	7.605	9.421	16.678	96.89	3	?	49
	$(ET)_3(HSO_4)_2$	7.633	9.440	16.607	96.87	3	130 K	49
	$(ET)_3(BF_4)_2$	7.654	9.496	16.398	96.09	3	150 K	50
	$(ET)_3(ClO_4)_2$	7.613	9.498	16.463	95.91	3	170 K	51
	$(ET)_3(BrO_4)_2$	7.670	9.550	16.686	96.13	3	210 K	52
	$(ET)_3Br_2(H_2O)_2$	7.718	9.587	16.167	98.91	3	185 K	53
312	α-$(ET)_3(NO_3)_2$	5.890	12.915	31.125	76.07	3	20 K	54
321	$(ET)_3Cl_{2.5}(H_5O_2)$	7.643	10.235	15.466	98.01	3	170 K	55
	$(ET)_3(HgBr_3)_2$	7.758	10.555	18.371	101.31	3	Insulator	56
321?	γ-$(ET)_3(ReO_4)_2$	8.409	9.295	16.124	97.05	3	Insulator	55
321?	$(ET)_3(IO_4)_2$	8.418	9.303	16.231	97.33	3	Insulator	56
3??	α-$(ET)_3(ReO_4)_2$	8.498	9.413	30.566	89.57	3	88 K	57
412	$(ET)_2(BF_4)(TCE)_{0.5}$	7.656	12.957	18.590	105.1	4	Metal	50
	$(ET)_2(ClO_4)(TCE)_{0.5}$	7.740	12.966	18.620	104.80	4	Metal	58
	$(ET)_2(FSO_3)(TCE)_{0.5}$	7.786	13.033	18.590	105.27	4	Metal	59
	$(ET)_2Cd_2I_6$	7.869	12.84	19.284	101.03	4	?	60
411	$(ET)_2Ni(CN)_4$	9.699	10.959	16.430	115.07	4	230 K	61,62
	$(ET)_2Pd(CN)_4$	9.735	10.997	16.546	115.15	4	250 K	63
	$(ET)_2Pt(CN)_4$	9.721	10.940	16.552	115.41	4	250 K	61,67
421	$(ET)_2Ni(CN)_4(H_2O)$	9.543	11.493	16.693	112.47	4	180 K	65
	$(ET)_2Pd(CN)_4(H_2O)$	9.562	11.529	16.685	112.29	4	80 K (SC)[e]	63
	$(ET)_2Pt(CN)_4(H_2O)$	9.563	11.514	16.704	112.29	4	80 K (SC)[e]	65
	$(ET)_2$(PrO-TCA)[d]	9.584	11.184	20.73	114.58	4	?	66
321×2[c]	$(ET)_3Cl_2(H_2O)_2$	11.228	13.905	15.929	97.08	6	100 K (SC)[e]	15
$3?\times2$	$(ET)_3NiCl_4H_2O$	9.016	16.269	16.696	90.81	6	Metal	68
$31?\times3$[c]	$(ET)_4H_2O[Fe(ox)_3]PhCN$	10.232	20.04	34.97	93.25	9	$T_{SC}=8.5$ K	69
$41?\times2$[c]	$(ET)_4Hg_2Cl_6(PhCl)$	12.586	16.049	18.984	106.02	8	Metal	70
	$(ET)_4Hg_2Br_6(PhCl)$	12.706	16.133	19.131	105.57	8	90 K	70
BO salts								
10	$(BO)_2Br(H_2O)_3$	4.023	5.340	16.774	98.42	1	Metal	71
	$(BO)_{2.4}I_3$	4.029	5.326	16.885	98.79	1	Metal	72
	$(BO)_{10}(CF)_4(H_2O)_3$[f]	4.031	5.342	17.225	98.59	1	Metal	73
	$(BO)_3Cu_2(NCS)_3$	4.237	5.273	33.481	97.94	1	$T_{SC}=1$ K	74
10×2[c]	$(BO)_2AuBr_2$	5.308	8.165	32.47	98.47	2	260 K	75
	$(BO)_2ClO_4$	5.340	8.069	33.43	98.25	2	200 K	75
	$(BO)_2PF_6$	5.358	8.080	17.04	97.91	2	Insulator	75
	$(BO)_2Ag(CN)_2$	4.035	10.234	16.76	98.88	2		76
	$(BO)_2$(HCHA)[g]	4.044	10.058	37.375	98.43	2	Metal	73
	$(BO)_4$(SQA)$(H_2O)_6$[h]	4.097	10.752	16.517	82.01	2	Metal	73
10×4[c]	$(BO)_2$(HCP)$(PhCN)_{0.2}$[i]	4.085	20.492	17.075	96.46	4	Insulator	73
20×2[c]	$(BO)_2ReO_4H_2O$	8.072	10.230	34.012	98.00	4	$T_{SC}=0.9$ K	77
40	$(BO)_2Br[MnBr_2(H_2O)_4](H_2O)$	6.182	14.001	20.099	100.21	4	Metal	73
50	$(BO)_4$(HCTMM)$(PhCN)_2$[j]	10.286	10.855	19.244	107.22	5	Metal	73
80	$(BO)CF_3SO_3(DO)_{0.5}$[k]	7.195	23.885	35.235	90.0	8	250 K	78

a) N: The number of ET molecules within a unit of the conducting sheet. b) DIA: diiodoacetylene. c) $\times2$ or $\times3$: Two or three fold periodicity in the transverese direction which originates from the anion lattice. d) PrO-TCA$^-$: 1,1,3,3-tetracyano-2-propoxy-2-propen-1-ide. e) SC: Superconducting under pressure. f) CF$^-$: tricyanomethanide $[C(CN)_3]^-$. g) HCHA^{2-}: chloranilate anion. h) SQA^{2-}: squarate anion. i) HCP^{2-}: tris(dicyanomethylene)cyclopropanediide. j) HCTMM^{2-}: hexacyanotrimethylenemethanediide.

Å interaction appears more frequently than the D = 3.3 Å interaction, the latter is regarded as a "dislocation." When D = 1.6 Å, the sulfur atom comes on the top of a carbon atom, then this is a kind of eclipsed configuration.

When the D = 0 Å and D = 3.3 Å interactions are represented as 0 and +, respectively, the ordinary β''-phase has an alignment represented as 0+0+0+$\cdots$ along the pseudo-stack. Similarly to the systematic nomenclature of the β-phase, we are able to designate the structure of β''-$(ET)_2AuBr_2$ as β''_{21}, where the first subscript 2 represents the periodicity in the pseudo-stacking direction, and the second subscript 1 stands for the number of the dislocations (+) within the repeating unit.

In this case, as shown in Fig. 11(a), two different structures, β''_{210} and β''_{211}, are possible, depending on the positions of the dislocations in the adjacent pseudo-stacks. Here *the third subscript designates the shift of the + position in the adjacent chains*. In the β''_{210}-phase the + signs are aligned horizontally, or in other words the dislocation runs parallel to the ϕ = 0° interaction. On the contrary, in the β''_{211}-phase the positions of the dislocation in the adjacent pseudo-stacks are displaced by one molecular unit. The ordinary β''-phase corresponds to β''_{211}.

An example of the β''_{210}-phase has been known in only one compound, $(ET)_2[N(SO_2CF_3)_2]$ (Table 3).[43] Recently an example of β''_{20}-phase, β''_{20}-$(ET)_2Cl(DIA)$ (DIA: diiodoacetylene), has been also found.[30] The third subscript is unnecessary when the second subscript is zero; since there is no dislocation, there is no need to designate the direction of its alignment. Another example of the β''_{20}-phase is an organic superconductor, $\beta''_{20\times2}$-$(BO)_2ReO_4H_2O$, although the transverse periodicity of this salt is doubled.[79]

Three-Fold Structures. Three-fold repetition like 00+00+00+$\cdots$ generates three modifications: β''_{310},β''_{311}, and β''_{312} (Fig. 11(a)). Here, in order to distinguish β''_{311} and β''_{312}, ϕ is chosen as shown in the left of Fig. 11(b), and the shift of the dislocation is counted in the positive ϕ direction.

Because many papers which report crystal structures contain neither the atomic coordinates nor the drawings of the conducting sheet structures, we have found difficulty in relating the actual crystal structures to one of the phases depicted in Fig. 11. However, if the structure type of one crystal is once identified definitely, we can determine the isostructural salts only by comparing their lattice constants.

In Table 3 are listed lattice constants of multiple β''-phase ET salts, where the lattice constants are arranged in the order of $a < b < c$. Since the molecule long axis c is approximately perpendicular to the conducting sheet, a and b make the lattice of the conducting sheet.

The area of the unit cell in the conducting sheet is given by $ab\sin\gamma$. Since one ET molecule occupies about 24 Å^2, we can estimate the number of ET molecules in the unit cell of the conducting sheet. This number is usually equal to the number of molecules in the repeating unit, namely the first subscript.

The β''_{311}-phase appears in $(ET)_3(ClO_4)_2$[51] and a large family of isostructural salts where the anions are interchangeable to FSO_4, HSO_4, BrO_4, BF_4, and $Br_2(H_2O)_2$. Because

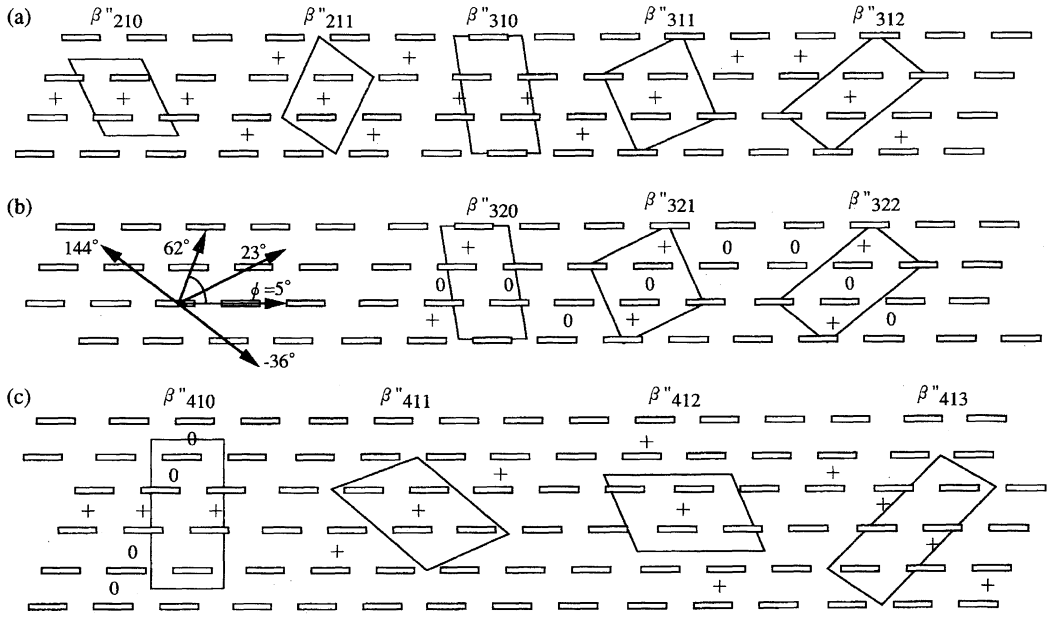

Fig. 11. Unit cells of multiple β''-phases. The unit cells are determined as follows; first the positions of + are decided according to the above rule. Once the + signs are placed, from the symmetry of the donor arrangement we can assume that some ET molecules are located on inversion centers. Sometimes inversion centers appear in the middle of the donor molecules. Almost all β''-phases have triclinic ($P\bar{1}$) symmetry. Choosing an inversion center as the origin, and connecting the equivalent inversion centers, we can draw the unit cell. As for a given structure there are several ways to choose the unit cell. Since in the usual crystallographic work the unit cell is so chosen as to make the lattice angles as close to 90° as possible, the lattices are depicted according to this rule.

we have taken β''_{311}-$(ET)_3(ClO_4)_2$ and β''_{412}-$(ET)_2X(TCE)_{0.5}$ as prototypes of β''-phases which are made up of the 0°–30°–60° interactions, we have preferably called these phases "ClO_4-type structure." However, if we follow the tradition that most phase names have been represented by Greek letters, all phases listed in Table 3 are, in a wide sense, classified as the β''-family.

These β''_{311}-salts undergo metal-insulator transitions around 150—200 K. Below the transition temperature, the magnetic susceptibility of β''_{311}-$(ET)_3(ClO_4)_2$ drops to a singlet state.[79] Under pressure, the transition temperature is gradually lowered.[80] The entries in Table 3 are aligned in the increasing order of b; in this order the metal-insulator transition temperature T_{MI} increases. (If instead of b we take another lattice constant a, the unit area of the conducting sheet $ab\sin\gamma$, or lattice volume V, the order changes for some occasions, but the basic tendency is the same.) As the b axis shrinks, the transfer integrals increase, and the M–I transition is suppressed. This tendency is in agreement with the pressure effect. Thus we can understand the systematic change of T_{MI} in view of chemical pressure.

Although the β''_{311}-phase appears in many salts, the β''_{312}-phase has been realized in only one salt, $(ET)_3(NO_3)_2$. To our knowledge there is no example of the β''_{310}-phase.

Three-fold structures containing two dislocations within a repeating unit like 0++0++0++ (β''_{32}), give three modifications, which are shown in Fig. 11(b). An example of the β''_{32}-structure is β''_{321}-$(ET)_3Cl_{2.5}(H_5O_2)$.[55] It should be noted that the lattice constants of this β''_{321}-phase are very close to those of the β''_{311}-phase. It is not easy to distinguish a β''_{32m}-phase from a β''_{31m}-phase only on the basis of the lattice constants, because the unit cells of β''_{320}, β''_{321}, and β''_{322} are essentially the same as those of β''_{310}, β''_{311}, and β''_{312}, respectively (Fig. 11), except for the small difference of the lattice angles caused by the difference of the number of dislocations. This comes from the fact that the β''_{32}-structures 0++0++ are generated from the β''_{31}-structures by exchanging + and 0.

Another comparatively well-known example of β''_{321}-structure is $\beta''_{321\times2}$-$(ET)_3Cl_2(H_2O)_2$ (Fig. 10(d)),[67] where the basic pattern is β''_{321}, but on account of the large anion unit ($Cl_4(H_2O)_4$), there is two-fold periodicity in the transverse direction, so that the structure is represented as $\beta''_{321\times2}$. A unit cell of this structure contains six ET molecules. This salt undergoes a metal-insulator transition around 100 K. The transition is suppressed under pressure, and a superconducting phase appears at 2 K under 16 kbar.[67]

Four-Fold Structures. The β''_{412}-structure with a stacking pattern 000+000+000+⋯ (Fig. 11(c)) has been observed in $(ET)_2X(TCE)_{0.5}$, where $X = ClO_4$,[58] BF_4,[50] FSO_3,[59] and TCE = 1,1,2-trichloroethane (or some other solvents).[81] These salts are metals down to low temperatures, but under a slow cooling condition a slight increase of resistance appears, accompanied by a drop of the magnetic susceptibility.[79]

Examples of the β''_{411}-structure are $(ET)_2M(CN)_4$ (M = Ni, Pd, and Pt).[61—63] These salts have comparatively high metal-insulator transition temperatures (230—250 K). When H_2O is incorporated with the same anions, the β''_{421}-structure, having the composition of $(ET)_2M(CN)_4H_2O$ (M = Ni, Pd, and Pt), is obtained.[63,65] The β''_{421}-salts undergo metal-insulator transitions at relatively low temperatures (80 K). The spin susceptibility shows a gradual decrease.[82] The $Pt(CN)_4$ and $Pd(CN)_4$ salts become superconducting under pressure.[63,65]

The lattice constants of these β''_{421}-phases are very close to those of the β''_{411}-phases; this is another example that *the second subscript is not easily decided only by comparing the lattice constants*. Although not shown in Fig. 11, β''_{42m}- and β''_{43m}-structures have almost the same unit cell as those of the β''_{41m}-structures shown in Fig. 11(c). The β''_{421}-phase involves the two-fold repetition of D like 0+0+0+⋯ as well as the β''_{211}-structure. However, this phase has four-fold periodicity owing to the anion arrangement.

BO Salts. Table 3 also lists BO salts. The β''-structure is the most frequently occurring structure (> 70%) in BO salts. Furtheremore *dislocations never appear in the BO-based β''-phases*; all second subscripts of the BO salts listed in Table 3 are zero. It has been pointed out that hydrogen bonds between the oxygen and the ethylene hydrogen atoms give rise to the extraordinarily strong preference of BO to the RA overlap.[71—75] The absence of dislocation is associated with the same structural rigidity as well.

Probably this is the reason that crystal structure analyses of many BO salts are unsuccessful owing to serious anion disorder. Because there is no dislocation, the donor sheet spreads monotonously within the conducting sheet; this leads to more than one possible pattern for the packing of the anions, which on the other hand needs a large repeating unit than that of a single donor. As a consequence, many BO salts have the same lattice constants, a = 4.2 Å, b = 5.3 Å, and γ = 98°; this is the minimal repeating unit which includes only one BO molecule with β''-type arrangement. $(BO)_3Cu_2(NCS)_3$ has these lattice constants, but the positions of anion atoms have not been determined.[74]

Because there is no dislocation, the modifications of BO-based β''-phases are able to be indicated by specifying only two periodicities: those along the pseudo-stacking (ϕ = 60°) and the transverse (ϕ = 0°) directions. For example $\beta''_{10\times2}$-phase has uniform (one-fold) periodicity along the pseudo-stacking (ϕ = 60°) direction and two-fold repeating unit in the transverse (ϕ = 0°) direction (Fig. 12(a)). Since in the β''_{10}-type salts a unit cell contains only one donor molecule, the lattice constants are very small: 4.2×5.3 Å^2 in the conducting sheet (Table 3).

Fermi Surface of β''-Phases. The Fermi surface of β''_{10}-$(BO)_2Br(H_2O)_3$ is composed of an ellipse, as shown in Fig. 12(b).[71] Since the overlap along the c axis (ϕ = 60° direction: 5.6×10^{-3}) is smaller than those in the ϕ = 0° and 30° directions (14.6 and -13.4×10^{-3} respectively), the ellipse is elongated along the k_c axis.

The β''_{10}-phase is a prototype of other β''-phase; *the Fermi surfaces of other β''-phases are generated from the Fermi surface of β''_{10}-phase* as follows. For instance, in the ordinary β''_{211}-$(ET)_2AuBr_2$, the repeating unit along the pseudo-stacking unit is doubled. In $(BO)_2Br(H_2O)_3$ this pseudo-stacking direction corresponds to the crystallographic c axis

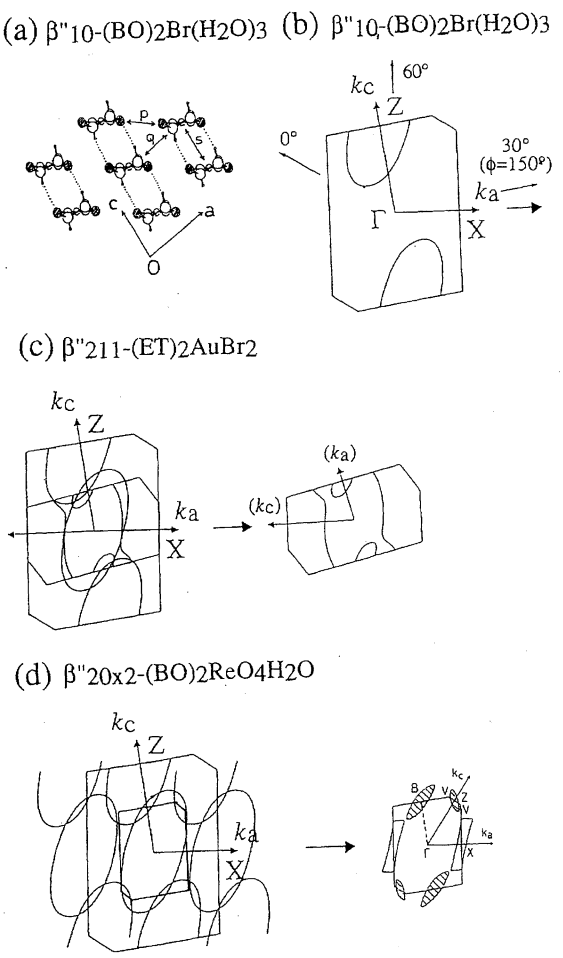

Fig. 12. Fermi surface and contraction of the first Brillouin zone in multiple β''-phases.

(Fig. 12(a)). As shown in Fig. 12(c), starting from the Brillouin zone of $(BO)_2Br(H_2O)_3$, another ellipse is put on the Γ point, and the Brillouin zone is made half along the k_c axis. The Fermi surface is succeedingly recombined at the points where the Fermi surfaces cross each other. Accordingly we can construct the Fermi surface of β''_{211}-$(ET)_2AuBr_2$; it is in good agreement with that obtained by the direct tight-binding calculation.[42]

As shown in Fig. 12(d), if we execute lattice doubling along the k_a axis as well as the k_c axis, we obtain the Fermi surface of $\beta''_{20\times2}$-$(BO)_2ReO_4H_2O$. There is experimental evidence (observation of Shubnikov-de Haas oscillations) about this semimetal-like Fermi surface.[84] Because the Fermi surfaces of other β''-phases are generated similarly, *multiple β''-phases* (particularly those having more than two-fold repeating unit in the pseudo-stacking (60°) direction) *usually have semimetal-like Fermi surfaces.* Such a band structure can be readily transformed into that of a semiconductor even by a slight change in the crystal structure. This is probably the origin of the metal-insulator transitions widely observed in the multiple β''-phases.

Third Subscript of the β''-Family. In the systematic nomenclature of the β''-family, we need the third subscript to distinguish the actually observed patterns, but in the β-phase we have used only two subscripts. In the β''-phase there is $\phi = 0°$ interaction, and the adjacent chain is able to be generated by a horizontal translation of the original chain. By contrast, in the β-phase the neighboring chain is shifted by a half molecular unit along the stacking axis (Fig. 8). As a result, the dislocations are automatically shifted (at least) this half molecular unit. The actual dislocations in the β-phase always run in this direction. Hence the third subscript is not necessary. In some highly multiple structures like β_{41}, several modifications are theoretically possible, but we have not known examples of such modifications.

When we investigate D values of the transverse ($\phi = 0°$ and 30°) directions in Fig. 10, we find that *all D values are approximately 1.6 Å*. This displacement is the optimal one for the $\phi = 0°$ and 30° interactions. This rule holds even if the structure has some dislocations.

β'-Phase

In contrast to the β''-phase, the β'-phase is, as shown in Fig. 5, composed of a stack of alternating RB and RA modes. The D values are 1.5 Å for RB and 4.0 Å for RA; the latter is very large and this is, strictly speaking, not the true RA mode. This structure is rather recognized as a "strongly dimerized" structure. Examples of this phase are listed in Table 2.

All these salts are low-conducting (0.01—0.03 $S\,cm^{-1}$) insulators even at room temperature. These salts have highly one-dimensional energy band structures.[30,31] Owing to the strong dimerization, the energy band splits to two. Because of the 2 : 1 composition, the whole energy band is three-quarters filled, and the upper band of the two is half-filled. The ground state of a one-dimensional half-filled band must be the Mott insulator. In other words, in real space one hole is localized on each dimer, so that the system is insulating on account of the Coulomb repulsion. Therefore a β'-phase salt exhibits the Bonner–Fisher-like magnetic susceptibility of a low-dimensional localized spin system with a broad maximum, and undergoes an antiferromagnetic transition around 20—30 K.[84]

Inclination from the Stacking Direction

The β-, β''-, θ-, and α-phases have stacking (or pseudo stacking) of the RB (or RA) overlap modes, but the molecular plane and the molecular long axis of each molecule are not perpendicular to the stacking direction. The inclination is closely related to the number of dislocations.

On account of the large D, the molecular plane of the β-phase is inclined with respect to the stacking direction (Figs. 7(c) and 13). When the unit cell length along the stacking direction is L, and the sum of D along this stack is $\sum D$, $\sin\delta = \sum D/L$ defines the angle of this inclination. Then $90° - \delta$ is equal to the angle between the stacking direction and the molecular long axis. *This angle is practically equal to the angle between the molecular plane and the conducting sheet.*

In Table 4 are listed δ values for representative ET salts. The δ values are also plotted in Fig. 13. The value 35° for the β-phase is among the largest for ET salts. A stack of the

Table 4. Angle δ between the Stacking Axis and the Molecular Long Axis

Compound	L /Å	D /Å	δ /°	Ref.
β-$(ET)_2I_3$	9.2	1.5+3.8=5.3	35	13
β'-$(ET)_2AuCl_2$	9.8	1.5+4.0=5.5	34	30
$\beta''_{321\times2}$-$(ET)_3Cl_2(H_2O)_2$	13.9	0.1+3.3+3.1=6.5	28	67
Reglar stack [(TTF)(TCNQ)]	(4.0)[a]	1.6	25	12
β''_{211}-$(ET)_2AuBr_2$	9.0	0.0+3.3=3.3	21	42
β''_{421}-$(ET)_2Pd(CN)_4H_2O$	9.7	0.1+3.3=3.4	20	63
β''_{311}-$(ET)_3(ClO_4)_2$	12.2	0.1+0.1+3.3=3.5	17	51
β''_{412}-$(ET)_2ClO_4TCE_{0.5}$	7.7	1.7+0.1=1.8	13	58
β''_{411}-$(ET)_2Pd(CN)_4$	19.2	0.2+3.6=3.8	11	63
θ-$(ET)_2RbZn(SCN)_4$	4.6	0.1+0.0=0.1	1	6
α-$(ET)_2KHg(SCN)_4$	10.1	0.1+0.1=0.2	1	85
α-$(ET)_2I_3$	9.2	0.1+0.1=0.2	1	86
$(TMTSF)_2X$	7.3	1.5−1.6=0.1	0	11

a) δ of the regular stack is obtained from the interplanar spacing 3.4 Å and D = 1.6 Å, as tan δ = 1.6/3.4.

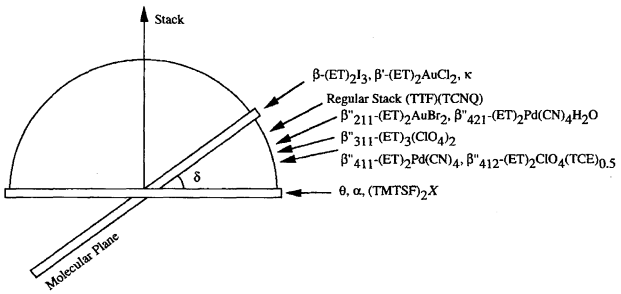

Fig. 13. Inclination of molecular plane δ with respect to the stacking direction. View along the molecular short axis.

β-phase involves an overlap (p2) with large D; thereby δ becomes very large. The δ value of a regular stack (Figs. 7(b) and 13) is 25°; by using the ordinary values of a regular stack, D = 1.6 Å and the interplanar spacing, Z = 3.4 Å, this value is obtained from the relation tan δ = 1.6/3.4. Because $\varkappa$-phase is also based on the RB mode, the molecular long axis is inclined by about 34° with respect to the conducting plane; this angle is comparable to the δ value in β-phases.

On the contrary, the RA mode does not have any slip along the molecular long axis (D = 0 Å), so that δ becomes nearly zero. As a consequence, θ and α-phases, composed of the RA mode, have nearly zero δ. This is because in the RA mode the steric hindrance of the ethylene group has been already resolved by the displacement along the molecular *short* axis, and no additional D along the molecular long axis is necessary.

In general, structures based on the RB mode, such as β and $\varkappa$-phases, have larger δ values than the standard value (25°) of the regular stack, but structures constructed from the RA mode, exemplified by θ, α, and β''-phases, have smaller δ values.

If β''-phases are purely made up of the RA mode with no dislocation, the δ values are approximately zero. This is realized in the BO-based salts. Most of actual ET-based β''-salts have some dislocations, and the δ values takes a value between 0° and 25°. As shown in Table 4, the δ values of β''-phases decrease with an increase of the periodicity (like $\beta''_{211} > \beta''_{311} > \beta''_{411}$). In other words, *$\delta$ increases with an increase of dislocations*. It is reasonable that the β''_{421}-phase and the β''_{211}-phase afford almost the same δ, because in both phases dislocations and the standard RA overlaps appear in the 1 : 1 ratio. $\beta''_{321\times2}$-$(ET)_3Cl_2(H_2O)_2$ has an extraordinarily high dislocation ratio, resulting in large δ = 28° (Table 4).

Not only the β'-phase, but also the β-phases and many of the ET-based β''-phases are significantly dimerized. This demonstrates the strong tendency of dimerization in ET. It should, however, be pointed out that the θ-phase has no dimerization.[7] Dimerization is unavoidable in the RB mode, but not necessary in the RA mode.

From this view, the modifications of the β''-phase illustrated in Fig. 11 are regarded as "trimerized" pseudo-stacks (for β''_{3m}-phases) and "tetramerized" pseudo-stacks (for β''_{4m}-phases). When a trimerized column is two-thirds filled as in $(ET)_3(ClO_4)_2$ and $(ET)_3Cl_2(H_2O)_2$, or when a tetramerized column is three-quarter filled as in $(ET)_2ClO_4(TCE)_{0.5}$ and $(ET)_2Pd(CN)_4$, the energy bands have to be either insulator or semimetal. Since these salts have a two-dimensional network of interaction, the energy bands are semimetal-like; this is a general characteristic of the multiple β''-phases. Accordingly we arrive at the same conclusion as Fig. 12.

Anion Size

The large variations of ET salts have been discussed in view of the size and shape of the anions. Although the β_{21}-phase occurs only when the anion is linear, other structures take place for various anion shapes. There is little correlation between the anion shape and the donor arrangement.

The size of the anion is a more important factor. The anion volumes are listed in Table 5. Here, although there have been several different definitions about the size of anions,[3,87] the anion volume V_A is defined from the equation: $V_{cell} = nV_D + mV_A$, where V_{cell} is the unit cell volume, V_D is the volume of an ET molecule (362 Å^3) estimated from the neutral ET crystal,[88] and n and m are the numbers of ET molecules and anions in a unit cell, respectively.

In general the β''-phase appears when the anion is small (< 100 Å^3). In particular the β''_{311}-phases with 3 : 2 composi-

Table 5. Anion Volume (Å^3) in ET Salts

β''-phase			
$(ET)_3(FSO_4)_2$	43	$(ET)_3(ClO_4)_2$	47
$(ET)_3(HSO)_4)_2$	47	$(ET)_3(BF_4)_2$	48
$(ET)_3(BrO_4)_2$	70	$(ET)_3(ReO_4)_2$	70
$(ET)_3(IO_4)_2$	72		
β''-$(ET)_2AuBr_2$	89	β''-$(ET)_2AuBrI$	102
$(ET)_2Ni(CN)_4$	46 (×2)	$(ET)_2Pt(CN)_4$	50 (×2)
$(ET)_2Pd(CN)_4$	56 (×2)	$(ET)_2Pt(C_2O_4)_2$	57 (×2)
$(ET)_3Cl_2(H_2O)_2$	65 (×2)[a]	$(ET)_2Pd(CN)_4(H_2O)$	97 (×2)
β'-phase			
β'-$(ET)_2AuCl_2$	76	β'-$(ET)_2ICl_2$	90
β'-$(ET)_2BrICl$	97		
$(ET)_3(ZnCl_4)_2$	110 (×2)	$(ET)_3(MnCl_4)_2$	121 (×2)
β-phase			
β-$(ET)_2IBr_2$	104	β-$(ET)_2I_2Br$	118
β-$(ET)_2AuI_2$	120	β-$(ET)_2I_3$	131
$(ET)_2InCl_4$	145	$(ET)_2InBr_4$	185
θ- and α-phases			
α-$(ET)_2Cu(SCN)_2$	111	θ-$(ET)_2I_3$	122
α-$(ET)_2I_3$	124	α-$(ET)_2KHg(SCN)_4$	274
α-$(ET)_2NH_4Hg(SCN)_4$	279	$(ET)_3CuBr_4$	99
$\varkappa$-phase			
$\varkappa$-$(ET)_2CuN(CN)_2Cl$	100	$\varkappa$-$(ET)_2CuN(CN)_2Br$	104
$\varkappa$-$(ET)_2Ag(CN)_2H_2O$	104	$\varkappa$-$(ET)_2CuN(CN)_2CN$	107
$\varkappa$-$(ET)_2I_3$	119	$\varkappa$-$(ET)_2Cu(SCN)_2$	123
$\varkappa$-$(ET)_2Hg_{2.89}Br_8$	181	$\varkappa$-$(ET)_2Ag(CF_3)_4TCE$	356
β-PF_6 (twisted dimer) structure			
β-$(ET)_2PF_6$	89	β-$(ET)_2AsF_6$	94
β-$(ET)_2SbF_6$	112		
α'-$(ET)_2Ag(CN)_2$	98	α'-$(ET)_2Au(CN)_2$	104
$(ET)_2FeCl_4$	154	$(ET)_2FeBr_4$	180

a) The values of divalent anions have been divided by two.

tion, like $(ET)_3(ClO_4)_2$, occur when the anion is smallest, in the range of 40—70 Å^3. The ordinary β''_{211}-phase is seen for slightly larger anions in the region of 90—100 Å^3. When the anion volume is still larger (> 100 Å^3), such phases as α, β, θ, and $\varkappa$ are realized.

In summary we have proposed a method to systematize various phases of ET-based organic conductors.

(1) The RA overlap mode as well as the ordinary RB overlap mode is the essential building block of ET-based salt. The RA and RB overlap modes correspond to the optimal overlaps of two molecules, and quantum chemically they are close to the maxima of overlap integrals at $\phi = 60°$ and 90°. By neglecting dislocations, different ways to pile up these elements lead to various families of structure types which are conventionally designated as β, β', β'', θ, α, and α''-phases.

(2) Anion packing as well as steric hindrance of the donor molecule give rise to dislocations. The introduction of dislocations makes a large number of multiple phases.

(3) The overlap integral is insensitive to D, and dislocations bring about no serious influence upon transfer integrals. Therefore the Fermi surfaces of the multiple phases are understood from the Fermi surface of the "parent" structures only by folding the first Brillouin zone.

Although the β- and β''-phases form a large number of structural modifications, the θ-, α, and $\varkappa$-phases give rise to essentially isostructural series. These phases will be treated in a separate paper.[7]

Method of Calculation

The atomic parameters of ET are taken from $(ET)_2CsCo(SCN)_4$.[89] The parameters are transformed so as to coincide with the coordinates of Fig. 1, and are then used for further calculations. This molecule has a two-fold axis along the molecular long axis. Molecular orbital calculation is carried out by the extended Hückel approximation.[90] The Slater exponents and the ionization potentials used in the present calculation are listed in Table 6. The Hückel parameters are standard ones except for that for the sulfur 3d orbital.[91] The ionization potential of sulfur 3d orbital has been chosen so as to give reasonable overlap integrals.[92] Since 1984 we have used these parameters,[8] so we shall use the same parameters. Later experiments have, however, indicated that these parameters overestimate the bandwidth by about 30—50% and the interstack

Table 6. Slater Exponents and Ionization Potentials Used for the Extended Hückel Calculations

Atomic	orbitals	Slater exponent	Ionization potential (eV)
H	1s	1.0	−13.6
C	2s	1.625	−21.4
C	2p	1.625	−11.4
S	3s	2.112	−20.0
S	3p	1.827	−11.0
S	3d	1.5	−5.44

interactions by about 20—40%.[93]

The coefficients of HOMO, so calculated, have been used for the calculations of intermolecular overlaps. The same Slater exponents are used for this calculation.

Transfer integrals, t, are obtained assuming $t = E \times S$, where S is the overlap integral and $E = -10$ eV. From these transfers we can calculate the band structure and the Fermi surface on the basis of the tight-binding approximation.

The molecular geometries of each interaction in an actual crystal are computed by a computer program written for this particular purpose. First the atomic coordinates are transformed to a rectangular system, then for a given molecule the vectors defining the molecular long and short axes are calculated. Second, for a neighboring molecule which interacts with the first one, the center of gravity is represented by the same rectangular coordinates, and X, Y, and Z in Fig. 1 are computed from the above vectors.

Appendix History of Nomenclature

Greek phase names like β, β', β'', θ, and $\varkappa$ in BEDT-TTF conductors are somewhat complicated. In order to illustrate how these nomenclatures have come to be used, some historical aspects will be described.

In the early study of BEDT-TTF salts, H. Kobayashi found that some BEDT-TTF salts had the same composition but different crystal structures. According to the tradition of crystallography, he distinguished these phases by Greek letters like α-(BEDT-TTF)$_2$PF$_6$ and β-(BEDT-TTF)$_2$PF$_6$.[94] Shortly after that, Schweitzer et al. and Shibaeva et al. independently reported different I_3^- salts with the same composition,[13,86] which we distinguished like α-(BEDT-TTF)$_2$I$_3$ and β-(BEDT-TTF)$_2$I$_3$. The latter salt had great importance and was investigated intensively in those days, because, although the first BEDT-TTF-based superconductor, (BEDT-TTF)$_2$ReO$_4$ (T_c = 2 K under 4 kbar) had already been reported,[20] this salt was the second ambient-pressure organic superconductor (T_c = 1.5 K) next to (TMTSF)$_2$ClO$_4$.[95] Furthermore, T_c rose as high as 8 K under a mild pressure (0.3 kbar).[96,97]

Succeedingly Shivaeba et al. reported several iodine salts: γ-(BEDT-TTF)$_3$(I$_3$)$_{2.5}$,[98] δ-(BEDT-TTF)I$_3$(TCE),[99] ε-(BEDT-TTF)I$_3$(I$_8$)$_{0.5}$,[100] ζ-(BEDT-TTF)$_2$I$_2$I$_8$,[101] and η-(BEDT-TTF)-I$_3$.[102] Although these phases had different compositions, they distinguished them by Greek letters. Subsequently Kobayashi and Kato discovered two organic superconductors: θ-(BEDT-TTF)$_2$I$_3$ and $\varkappa$-(BEDT-TTF)$_2$I$_3$.[103,104] The compositions of these phases were the same as the first α and β phases. The Greek letter ι (iota) appears between θ and $\varkappa$, but Kobayashi skipped this Greek letter on account of its shape and other usages. Up to this period the Greek letters had been used in order to distinguish different phases with the same counter anion.

Along with the discoveries of many crystal phases, the Russian group and particularly the Argonne group developed a versatile method for obtaining new organic superconductors. By changing the counter anion slightly, but not changing the shape and the approximate size, they obtained a series of isostructural superconductors. For example they replaced the I_3^- anion of β-(BEDT-TTF)$_2$I$_3$ by IBr_2^-,[17] I_2Br^-,[16] and AuI_2^-,[15] generating new organic superconductors with essentially the same structure. Because these phases had the same structure except the slight volume change coming from the substitution of one or some of the iodine atoms by other atoms, all these phases were called β-phases like β-(BEDT-TTF)$_2$AuI$_2$, although α-(BEDT-TTF)$_2$AuI$_2$ had not yet been known.

In the course of explorations oriented in this direction, when the linear anions were still shorter, slightly different phases were found, which were called β'-phase (for ICl_2^-,[31] $IClBr^-$,[32] and $AuCl_2^-$ [30]) and β''-phase (for $AuBr_2^-$ [42] $AuBrI^-$,[45] and ICl_2^- [44]) (Fig. 14). In these phases, the RB mode of the β-phase is replaced by the RA mode one by one. As a consequence the unit cell length along the stacking direction contracts, in accordance with the shorter anions.

In those days these phases, which incorporated two BEDT-TTF molecules in a unit cell, were generally regarded as β-phase in a wide sense. The number of primes ($'$) designated the number of the RA overlap modes in a unit cell. However, many multiple phases have been found in the subsequent investigations, so that today we consider that the basic stacking pattern (or equivalently the environment of one molecule) is more essential, as extensively discussed in the present paper. Thus we shall use these names: β, β', and β'' for indicating these basic stacking patterns.

After Kobayashi found $\varkappa$-(BEDT-TTF)$_2$I$_3$, Urayama and Saito discovered a new organic superconductor, $\varkappa$-(BEDT-TTF)$_2$Cu-(SCN)$_2$, which underwent a superconducting transition at 10.4 K; this was the record high in those days.[105] The anion structure of this phase is different from $\varkappa$-(BEDT-TTF)$_2$I$_3$; the latter is made up of discrete I_3^-, but the former has an infinite network of Cu-(SCN)$_2^-$. Even the space groups are different in these phases. Nonetheless, because the basic donor arrangement is similar, the Cu(SCN)$_2$ salt was called $\varkappa$-phase. Succeedingly, many $\varkappa$-phase compounds were prepared; they have a rich variety of anion structures, but the donor arrangements are essentially the same. Many of the BEDT-TTF-based $\varkappa$-phases are superconductors, including $\varkappa$-(BEDT-TTF)$_2$Cu[N(CN)$_2$]Cl, which shows the highest T_c to date besides the fullerene compounds.[5]

Therefore *in the early days the Greek symbols were used to distinguish structurally different phases with the same anion and composition.* However, *gradually general names of structure types were getting more and more desired, so the Greek symbols of some*

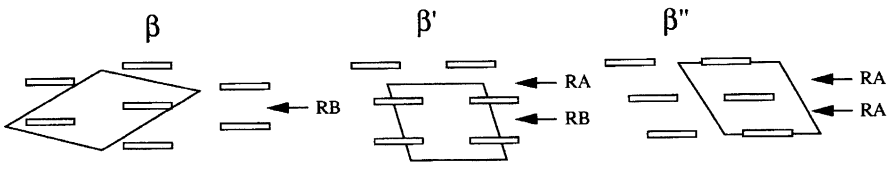

Fig. 14. Donor arrangements of β-, β'-, and β''-phases.

typical phases came to be used in order to identify these structure types. From today's point of view, we should use the phase names according to the second principle as much as possible. Furthermore we will generalize the phase names so as to apply them to groups of similar structures; examples are generalized β- and β''-phases discussed in the present paper. On the other hand we could not change the historical usage; this is the reason for nonsystematic naming.

Beno et al. has named α'-(BEDT-TTF)$_2$AuBr$_2$ as α'-phase,[106] but this phase has no structural relation to the well-known α-phase. In this salt, the molecular long axes of BEDT-TTF molecules are not parallel to each other. In this respect the α'-phase has a close resemblance to β-(BEDT-TTF)$_2$PF$_6$. This salt is named in order to be distinguished from α-(BEDT-TTF)$_2$PF$_6$, so that this salt is not related to the usual β-phase. Since δ-(BEDT-TTF)$_2$AuI$_2$ and δ-(BEDT-TTF)$_2$AuBr$_2$ have basically the same donor arrangement as β-(BEDT-TTF)$_2$PF$_6$, we shall call this structure δ-phase. In the δ-phase four molecules make the repeating unit along the stacking direction, whereas the α'-phase has a two-molecular repeating unit. The α' and δ-phases will be discussed in the third paper of this series.

H. Mori has designated α''-(BEDT-TTF)$_2$CsHg(SCN)$_4$ as α''-phase.[29] As shown in Fig. 5, α''-phase is derived from θ-phase rather than α-phase. From this view this phase would be preferably called θ'-phase. The Russian group, however, has also used this name,[107] so that this phase will be called α''-phase.

(BEDT-TTF)$_2$I$_3$ makes most major phases such as α, β, θ, and $\varkappa$. Thus we may regard that *the phase names are taken from the structures of (BEDT-TTF)$_2$I$_3$*. From γ to η, there are no isostructural salts, so these symbols are seldom used. (BEDT-TTF)$_2$AuBr$_2$ also forms a rich variety of phases: α', β'', and δ. If we add these phases to the list of (BEDT-TTF)$_2$I$_3$ phases, we can cover most major phases.

Since these phases were originally named in the order of discovery, the phases represented by the earlier symbols, α and β tend to appear as the major products under the usual conditions of electrochemical crystal growth. For example, in the elctrocrystallization with I_3^-, α-(BEDT-TTF)$_2$I$_3$ is the major product, β-(BEDT-TTF)$_2$I$_3$ is obtained as a minor product, and θ- and $\varkappa$-phases are obtained only under special conditions. α'-(BEDT-TTF)$_2$AuBr$_2$ is also the major product of this combination, and β''-(BEDT-TTF)$_2$AuBr$_2$ is obtained as a minor product.

The author is grateful to Dr. U. Geiser; his report about a θ-/β''-disordered phase has given an important clue to this work. The author is also grateful to Professor R. Kato and Dr. H. Yamamoto for valuable discussion about the β''-phases and for sending him the results of β''-(ET)$_2$Cl(DIA) and (ET)$_3$Cl(pBIB) prior to the publication.

References

1) D. Jérome, A. Mazaud, M. Ribault, and K. Bechgaard, *J. Phys.*, **41**, L95 (1980).

2) T. Ishiguro and K. Yamaji, "Organic Superconductors," Springer, Berlin (1990).

3) J. M. Williams, J. R. Ferraro, R. J. Thorn, K. D. Carlson, U. Geiser, H. H. Wang, A. M. Kini, and M.-H. Whangbo, "Organic Superconductors," Prentice Hall, New Jersey (1992).

4) J. Wosnitza, "Fermi Surfaces of Low-Dimensional Organic Metals and Superconductors," Springer, Berlin (1996).

5) J. M. Williams, A. M. Kini, H. H. Wang, K. D. Carlson, U. Geiser, L. K. Montgomery, G. J. Pyrka, D. M. Watkins, J. M. Kommers, S. J. Boryshuk, A. V. Strieby Crouch, W. K. Kwok, J. E. Schirber, D. J. Overmyer, D. Jung, and M.-H. Whangbo, *Inorg. Chem.*, **29**, 3272 (1990).

6) T. J. Kistenmacher, *Isr. J. Chem.*, **27**, 327 (1986).

7) T. Mori, in preparation.

8) T. Mori, A. Kobayashi, Y. Sasaki, H. Kobayashi, G. Saito, and H. Inokuchi, *Bull. Chem. Soc. Jpn.*, **57**, 627 (1984).

9) J. P. Lowe, *J. Am. Chem. Soc.*, **102**, 1262 (1980).

10) U. Geiser, J. A. Schlueter, H. H. Wang, A. M. Kini, J. D. Dudek, and J. M. Williams, private communication.

11) N. Thorup, G. Rindorf, H. Soling, and K. Bechgaard, *Acta Crystallogr. Sect. B*, **B37**, 1236 (1981).

12) T. J. Kistenmacher, T. E. Phillips, and D. O. Cowan, *Acta Crystallogr., Sect. B*, **B30**, 763 (1974).

13) T. Mori, A. Kobayashi, T. Sasaki, H. Kobayashi, G. Saito, and H. Inokuchi, *Chem. Lett.*, **1984**, 957; R. P. Shibaeva, V. F. Kaminskii, and V. K. Bel'skii, *Sov. Phys. Crystallogr.*, **29**, 638 (1984).

14) A. Kawamoto, J. Tanaka, and M. Tanaka, *Acta Crystallogr., Sect. C*, **C43**, 205 (1987).

15) H. H. Wang, M. A. Beno, U. Geiser, M. A. Firestone, K. S. Webb, L. Nunez, G. W. Crabtree, K. D. Carlson, J. M. Williams, L. J. Azevedo, J. F. Kwok, and J. E. Schirber, *Inorg. Chem.*, **24**, 2465 (1985).

16) T. J. Emge, H. H. Wang, M. A. Beno, P. C. W. Leung, M. A. Firestone, H. C. Jenkins, J. D. Cook, K. D. Carlson, J. M. Williams, E. L. Venturini, L. J. Azevedo, and J. E. Schirber, *Inorg. Chem.*, **24**, 1736 (1985); H. Kobayashi, R. Kato, A. Kobayashi, G. Saito, M. Tokumoto, H. Anzai, and T. Ishiguro, *Chem. Lett.*, **1985**, 1293.

17) J. M. Williams, H. H. Wang, M. A. Beno, T. J. Emge, L. M. Sowa, P. T. Copps, F. Behroozi, L. N. Hall, K. D. Carlson, and G. W. Crabtree, *Inorg. Chem.*, **23**, 3839 (1994); E. B. Yagubskii, I. F. Schegolev, R. P. Shibaeva, D. N. Fedutin, L. P. Rozenberg, E. M. Sogomonyan, R. M. Lyubovskaya, V. N. Laukhin, A. A. Igna'ev, A. V. Zvarykina, and L. I. Bravov, *JETP Lett.*, **42**, 206 (1985).

18) U. Geiser, B. A. Anderson, A. Murray, C. M. Pipan, C. A. Rohl, B. A. Vogt, H. H. Wang, J. M. Williams, D. B. Kang, and M.-H. Whangbo, *Mol. Cryst. Liq. Cryst.*, **181**, 105 (1990).

19) H. Kobayashi, R. Kato, T. Mori, A. Kobayashi, Y. Sasaki, G. Saito, and H. Inokuchi, *Chem. Lett.*, **1983**, 759.

20) J. M. Williams, M. A. Beno, H. H. Wang, P. E. Reed, L. J. Azevedo, and J. E. Schirber, *Inorg. Chem.*, **23**, 1790 (1984).

21) X. Wang, C. Ge, X. Xing, P. Wang, D. Zhang, P. Wu, and D. Zhu, *Synth. Met.*, **39**, 355 (1991); **49**, 253 (1992).

22) H. M. Yamamoto, J. Yamaura, and R. Kato, *J. Mater. Chem.*, **8**, 15 (1998).

23) M. A. Beno, D. D. Cox, J. M. Williams, and J. F. Kwak, *Acta Crystallogr., Sect. C*, **C40**, 1334 (1984).

24) U. Geiser, H. H. Wang, J. A. Schlueter, S. L. Hallenbeck, T. J. Allen, M. Y. Chen, H.-C. I. Kao, K. D. Carlson, L. E. Gerdom, and J. M. Williams, *Acta Crystallogr., Sect. C*, **C44**, 1544 (1988).

25) Y.-K. Yan, D. M. P. Mingos, D. J. Williams, and M. Kurmoo, *J. Chem. Soc., Dalton Trans.*, **1995**, 3221.

26) T. Mori, P. Wang, K. Imaeda, T. Enoki, and H. Inokuchi, *Solid State Commun.*, **64**, 733 (1987).

27) R. N. Lyubovskaya, S. A. Konovalikhin, O. A. Dyachenko, and R. B. Lyubovskii, *Synth. Met.*, **70**, 1145 (1995).

28) E. Coronado, J. R. Galan-Mascaros, C. Gimenez-Saiz, and C. J. Gomez-Garcia, *Adv. Mater.*, **8**, 801 (1996).

29) H. Mori, S. Tanaka, T. Mori, Y. Maruyama, H. Inokuchi,

and G. Saito, *Solid State Commun.*, **78**, 49 (1991).

30) T. Mori and H. Inokuchi, *Solid State Commun.*, **62**, 525 (1987).

31) H. Kobayashi, R. Kato, A. Kobayashi, G. Saito, M. Tokumoto, H. Anzai, and T. Ishiguro, *Chem. Lett.*, **1986**, 89.

32) T. J. Emge, H. H. Wang, P. C. W. Leung, P. R. Rust, J. D. Cook, P. L. Jackson, K. D. Carlson, J. M. Williams, M.-H. Whangbo, E. L. Venturini, J. E. Schirber, L. J. Azevedo, and J. R. Ferraro, *J. Am. Chem. Soc.*, **108**, 695 (1986).

33) T. Mori and H. Inokuchi, *Solid State Commun.*, **59**, 355 (1986).

34) R. P. Shibaeva, R. M. Lyubovskaya, V. E. Korotkov, N. D. Kushch, E. B. Yagubskii, and M. K. Makova, *Synth. Met.*, **27**, A457 (1988).

35) T. Mori and H. Inokuchi, *Bull. Chem. Soc. Jpn.*, **61**, 591 (1988).

36) H. Kobayashi, T. Udagawa, H. Tomita, K. Bun, T. Naito, and A. Kobayashi, *Chem. Lett.*, **1993**, 1559.

37) H. Kobayashi, H. Tomita, T. Naito, A. Kobayashi, F. Sakai, T. Watanabe, and P. Cassoux, *J. Am. Chem. Soc.*, **118**, 369 (1996).

38) K. Carneiro, J. C. Scott, and E. M. Engler, *Solid State Commun.*, **50**, 477 (1984)

39) S. S. P. Parkin, E. M. Engler, R. R. Schumaker, R. Lagier, V. Y. Lee, J. C. Scott, and R. L. Greene, *Phys. Rev. Lett.*, **50**, 270 (1983); S. S. P. Parkin, E. M. Engler, R. R. Schumaker, R. Lagier, V. Y. Lee, J. Voiron, K. Carneiro, J. C. Scott, and R. L. Greene, *J. Phys.*, **44**, C3-791 (1983).

40) Y. Misaki, K. Kawakami, H. Fujiwara, T. Yamabe, T. Mori, H. Mori, and S. Tanaka, *Chem. Lett.*, **1995**, 1125.

41) K. Oshima, T. Mori, H. Inokuchi, H. Urayama, H. Yamochi, and G. Saito, *Phys. Rev. B*, **38**, 938 (1988).

42) T. Mori, F. Sakai, G. Saito, and H. Inokuchi, *Chem. Lett.*, **1986**, 1037.

43) H. H. Wang, U. Geiser, M. E. Kelly, M. L. Vanzile, A. J. Skulan, J. M. Williams, J. A. Schlueter, A. M. Kini, S. A. Sirchio, and L. K. Montgomery, *Mol. Cryst. Liq. Cryst.*, **284**, 427 (1996).

44) A. Ugawa, Y. Okawa, K. Yakushi, H. Kuroda, A. Kawamoto, J. Tanaka, M. Tanaka, Y. Nogami, S. Kagoshima, K. Murata, and T. Ishiguro, *Synth. Met.*, **27**, A407 (1988).

45) H. Yamamoto, J. Yamaura, and R. Kato, *J. Mat. Chem.* in press; A. Ugawa, K. Yakushi, H. Kuroda, A. Kawamoto, and J. Tanaka, *Chem. Lett.*, **1986**, 1875.

46) U. Geiser, J. A. Schlueter, J. D. Dudek, and J. M. Williams, *Mol. Cryst. Liq. Cryst.*, **284**, 203 (1996); U. Geiser, H. H. Wang, J. A. Schlueter, J. M. Williams, J. L. Smart, A. C. Cooper, S. K. Kumar, M. Caleca, J. D. Dudek, K. D. Carlson, J. Ren, M.-H. Whangbo, J. E. Schirber, and W. R. Bayless, *Inorg. Chem.*, **33**, 5101 (1994).

47) U. Geiser, J. A. Schlueter, H. H. Wang, A. M. Kini, J. M. Williams, P. P. Sche, H. I. Zakowicz, M. L. VanZile, J. D. Dudek, P. G. Nixon, R. W. Winter, G. L. Gard, J. Ren, and M.-H. Whangbo, *J. Am. Chem. Soc.*, **118**, 9996 (1996).

48) P. Day, M. Kurmoo, T. Mallah, I. R. Marsden, R. H. Friend, F. L. Pratt, W. Hayes, D. Chasseau, J. Gaultier, G. Bravic, and L. Ducasse, *J. Am. Chem. Soc.*, **114**, 10722 (1992).

49) L. C. Porter, H. H. Wang, M. M. Miller, and J. M. Williams, *Acta Crystallogr., Sect. C*, **C43**, 2201 (1987); N. D. Kushch, E. B. Yagubskii, V. E. Korotkov, R. P. Shibaeva, L. I. Buravov, A. V. Zvarykina, V. N. Laukhin, and A. G. Khomenko, *Synth. Met.*, **42**, 2131 (1991).

50) S. S. P. Parkin, E. M. Engler, V. Y. Lee, and R. R. Schumaker, *Mol. Cryst. Liq. Cryst.*, **119**, 375 (1985).

51) H. Kobayashi, R. Kato, T. Mori, A. Kobayashi, Y. Sasaki, G. Saito, T. Enoki, and H. Inokuchi, *Chem. Lett.*, **1984**, 179.

52) M. A. Beno, G. S. Blackmen, P. C. W. Leung, K. D. Carlson, P. T. Copps, and J. M. Williams, *Mol. Cryst. Liq. Cryst.*, **119**, 409 (1985).

53) H. Urayama, G. Saito, A. Kawamoto, and J. Tanaka, *Chem. Lett.*, **1987**, 1753.

54) A. Weber, H. Endres, H. J. Keller, E. Gogu, I. Heinen, K. Bender, and D. Schweizer, *Z. Naturforsch., Teil B*, **40B**, 1658 (1985).

55) H. Mori, I. Hirabayashi, S. Tanaka, and Y. Maruyama, *Bull. Chem. Soc. Jpn.*, **66**, 2156 (1993).

56) H. Muller, H. P. Fritz, C.-P. Heidemann, F. Gross, H. Veith, A. Lerf, K. Andres, H. Fuchs, K. Polborn, and W. Abriel, *Synth. Met.*, **27**, A257 (1988).

57) K. Carneiro, J. C. Scott, and E. M. Engler, *Solid State Commun.*, **50**, 477 (1984); H. Kanbara, H. Tajima, S. Aratani, K. Yakushi, H. Kuroda, G. Saito, A. Kawamoto, and J. Tanaka, *Chem. Lett.*, **1986**, 437.

58) H. Kobayashi, A. Kobayashi, Y. Sasaki, G. Saito, T. Enoki, and H. Inokuchi, *J. Am. Chem. Soc.*, **105**, 297 (1983).

59) D. D. Cox, G. A. Ball, A. S. Alonso, and J. M. Williams, *Inorg. Synth.*, **26**, 393 (1989).

60) E. I. Zhilyaeva, R. N. Lyubovskaya, O. A. Dyachenko, T. G. Takhirov, V. V. Crisenko, and S. V. Konovalikhin, *Synth. Met.*, **42**, 2247 (1991).

61) L. Ouahab, J. Padiou, D. Grandjean, C. Garrigou-Lagrange, P. Delhaes, and M. Bencharif, *J. Chem. Soc., Chem. Commun.*, **1989**, 1038.

62) M. Tanaka, H. Takeuchi, A. Kawamoto, J. Tanaka, T. Enoki, K. Suzuki, K. Imaeda, and H. Inokuchi, in "The Physics and Chemistry of Organic Superconductors," ed by G. Saito and S. Kagoshima, Springer, New York (1990), p. 298.

63) T. Mori, K. Kato, Y. Maruyama, H. Inokuchi, H. Mori, I. Hirabayashi, and S. Tanaka, *Solid State Commun.*, **82**, 177 (1992).

64) R. P. Shibaeva, R. M. Lobkovskaya, V. E. Korotkov, N. D. Kushch, E. B. Yagubskii, and M. K. Makova, *Synth. Met.*, **27**, A457 (1988); R. M. Lobkovskaya, N. D. Kushch, R. P. Shibaeva, E. B. Yagubskii, and M. A. Simonov, *Sov. Phys. Crystallogr.*, **34**, 698 (1989).

65) H. Mori, I. Hirabayashi, S. Tanaka, T. Mori, Y. Maruyama, and H. Inokuchi, *Solid State Commun.*, **80**, 411 (1991).

66) H. Yamochi, C. Tada, S. Sekizaki, G. Saito, M. Kusunoki, and K. Sakaguchi, *Mol. Cryst. Liq. Cryst.*, **284**, 379 (1996).

67) T. Mori and H. Inokuchi, *Chem. Lett.*, **1987**, 1657; M. J. Rosseinsky, M. Kurmoo, D. R. Talham, P. Day, D. Chasseau, and D. Watkin, *J. Chem. Soc., Chem. Commun.*, **1988**, 88; T. Mori and H. Inokuchi, *Solid State Commun.*, **82**, 525 (1987).

68) J. C. Fitzmaurice, A. M. Slawin, D. J. Williams, and J. D. Woollins, *J. Chem. Soc., Chem. Commun.*, **1993**, 1479.

69) M. Kurmoo, A. W. Graham, P. Day, S. J. Coles, M. B. Hursthouse, J. L. Caulfield, J. Singleton, F. L. Pratt, W. Hayes, L. Ducasse, and P. Guionneau, *J. Am. Chem. Soc.*, **117**, 12209 (1995).

70) R. N. Lyubovskaya, O. A. Dyachenko, V. V. Gritsenko, S. G. Mkoyan, L. O. Atovmyan, R. B. Lyubovskii, V. N. Laukhin, A. V. Zvarykina, and A. G. Khomenko, *Synth. Met.*, **42**, 1907 (1991); R. P. Shivaeba and L. P. Rozenberg, *Kristallografiya*, **33**, 1402 (1988); M. Z. Aldosina, L. M. Goldenberg, E. I. Zhilyaeva, R. N. Lyubovskaya, T. G. Takhirav, O. A. Dyachenko, L. O. Atovmyan, and R. B. Lyubovskii, *Mater. Sci.*, **14**, 45 (1988).

71) S. Horiuchi, H. Yamochi, G. Saito, J. K. Jeszka, A. Tracz, A. Sroczynska, and J. Ulanski, *Mol. Cryst. Liq. Cryst.*, **296**, 365

(1997).

72) F. Wudl, H. Yamochi, T. Suzuki, H. Isotalo, C. Fite, H. Kasmai, K. Liou, and G. Srdanov, *J. Am. Chem. Soc.*, **112**, 2461 (1990); I. Cisarova, K. Maly, X. Bu, A. Frost-Jensen, P. Sommer-Larsen, and P. Coppens, *Chem. Mater.*, **3**, 647 (1991).

73) S. Horiuchi, H. Yamochi, G. Saito, K. Sakaguchi, and M. Kusunoki, *J. Am. Chem. Soc.*, **118**, 8604 (1996); H. Yamochi, K. Tsutsumi, G. Saito, to be published.

74) M. A. Beno, H. H. Wang, A. M. Kini, K. D. Carlson, U. Geiser, W. K. Kwok, J. E. Thompson, J. M. Williams, J. Ren, and M.-H. Whangbo, *Inorg. Chem.*, **29**, 1599 (1990).

75) M. A. Beno, H. H. Wang, K. D. Carlson, A. M. Kini, G. M. Frankenbach, J. R. Ferraro, N. Larson, G. D. MaCabe, J. Thompson, C. Purnama, M. Vashon, J. M. Williams, D. Jung, and M.-H. Whangbo, *Mol. Cryst. Liq. Cryst.*, **181**, 145 (1990).

76) R. Li, V. Petricek, I. Cisarova, and P. Coppens, *Acta Crystallogr., Sect. B*, **B51**, 798 (1995).

77) S. Kahlich, D. Schweitzer, I. Heinen, S. E. Lan, B. Nuber, H. Keller, K. Winzer, and H. W. Herberg, *Solid State Commun.*, **80**, 191 (1991); S. Kahlich, D. Schweitzer, C. Rovia, J. A. Paradis, M.-H. Whangbo, I. Heinen, H. Keller, B. Nuber, P. Bele, H. Brunner, and R. P. Shivaeba, *Z. Phys., B*, **B94**, 39 (1994); L. I. Buravov, A. G. Khomenko, K. D. Kushch, V. N. Laukhin, A. I. Schegolev, E. B. Yagubskii, L. P. Rozenberg, and R. P. Shibaeva, *J. Phys. I*, **2**, 529 (1992).

78) M. Fettouhi, L. Ouahab, D. Serhani, J.-M. Fabre, L. Ducasse, J. Amiell, R. Canet, and P. Delhaes, *J. Mater. Chem.*, **3**, 1101 (1993).

79) M. Kobayashi, T. Enoki, K. Imaeda, H. Inokuchi, and G. Saito, *Phys. Rev. B*, **36**, 1457 (1987).

80) K. Imaeda, T. Enoki, G. Saito, and H. Inokuchi, *Bull. Chem. Soc. Jpn.*, **61**, 3332 (1988).

81) A. Miyazaki, I. Ichikawa, T. Enoki, and G. Saito, *Bull. Chem. Soc. Jpn.*, **70**, 2647 (1997).

82) T. Mori, K. Kato, Y. Maruyama, H. Inokuchi, H. Mori, I. Hirabayashi, and S. Tanaka, *Synth. Met.*, **56**, 2911 (1993).

83) S. Kahlich, D. Schweitzer, P. Auban-Senzier, D. Jerome, and H. Keller, *Solid State Commun.*, **80**, 191 (1991); L. I. Bravov, A. G. Khomenko, N. D. Kushch, V. N. Laukhin, A. I. Schegolev, E. B. Yagubskii, L. P. Rozenberg, and R. P. Shibaeva, *J. Phys. I*, **2**, 529 (1992).

84) N. Yoneyama, A. Miyazaki, T. Enoki, and G. Saito, *Synth. Met.*, **86**, 2029 (1997).

85) H. Mori, S. Tanaka, M. Oshima, G. Saito, T. Mori, Y. Maruyama, and H. Inokuchi, *Bull. Chem. Soc. Jpn.*, **63**, 2183 (1990).

86) K. Bender, I. Hennig, D. Schweizer, K. Dietz, H. Endres, and H. J. Keller, *Mol. Cryst. Liq. Cryst.*, **108**, 359 (1984).

87) H. Yamochi, T. Komatsu, N. Matsukawa, G. Saito, T. Mori, M. Kusumoto, and K. Sakaguchi, *J. Am. Chem. Soc.*, **115**, 11319 (1993).

88) H. Kobayashi, A. Kobayashi, Y. Sasaki, G. Saito, and H. Inokuchi, *Bull. Chem. Soc. Jpn.*, **59**, 301 (1986).

89) H. Mori, S. Tanaka, T. Mori, and Y. Maruyama, *Bull. Chem. Soc. Jpn.*, **68**, 1136 (1995).

90) R. Hoffman, *J. Chem. Phys.*, **39**, 1397 (1963).

91) A. J. Berlinsky, J. F. Carolan, and L. Weiler, *Solid State Commun.*, **15**, 795 (1974).

92) T. Mori, A. Kobayashi, Y. Sasaki, and H. Kobayashi, *Chem. Lett.*, **1982**, 1923.

93) H. Tajima, K. Yakushi, H. Kuroda, and G. Saito, *Solid State Commun.*, **56**, 159 (1985).

94) H. Kobayashi, R. Kato, T. Mori, A. Kobayashi, Y. Sasaki, G. Saito, and H. Inokuchi, *Chem. Lett.*, **1983**, 759.

95) K. Bechgaard, K. Carneiro, M. Olsen, F. B. Rasmussen, and C. S. Jacobsen, *Phys. Rev. Lett.*, **46**, 852 (1981).

96) K. Morata, M. Tokumoto, H. Anzai, H. Bando, G. Saito, K. Kajimura, and T. Ishiguro, *J. Phys. Soc. Jpn.*, **54**, 1236 (1985).

97) V. N. Laukhin, E. E. Kostyuchenko, Yu. V. Sushuko, I. F. Shchegolev, and E. B. Yagubskii, *JETP Lett.*, **41**, 81 (1985).

98) R. P. Shivaeba, V. F. Kaminskii, and E. B. Yagubskii, *Mol. Cryst. Liq. Cryst.*, **119**, 361 (1985).

99) R. P. Shivaeba, R. M. Lobkovskaya, V. F. Kaminskii, S. V. Lindeman, and E. B. Yagubskii, *Sov. Phys. Crystallogr.*, **31**, 546 (1986).

100) R. P. Shivaeba, R. M. Lobkovskaya, E. B. Yagubskii, and E. E. Kortyuchenko, *Sov. Phys. Crystallogr.*, **31**, 267 (1986).

101) R. P. Shivaeba, R. M. Lobkovskaya, E. B. Yagubskii, and E. E. Kortyuchenko, *Sov. Phys. Crystallogr.*, **31**, 657 (1986).

102) R. P. Shivaeba, R. M. Lobkovskaya, E. B. Yagubskii, and E. E. Laukhina, *Sov. Phys. Crystallogr.*, **31**, 530 (1986).

103) H. Kobayashi, R. Kato, A. Kobayashi, Y. Nishio, K. Kajita, and W. Sasaki, *Chem. Lett.*, **1987**, 789 and 833.

104) R. Kato, H. Kobayashi, A. Kobayashi, S. Moriyama, Y. Nishio, K. Kajita, and W. Sasaki, *Chem. Lett.*, **1987**, 507 and 459.

105) H. Urayama, H. Yamochi, G. Saito, S. Sato, A. Kawamoto, J. Tanaka, T. Mori, Y. Maruyama, and H. Inokuchi, *Chem. Lett.*, **1988**, 463.

106) M. A. Beno, M. A. Firestone, P. C. W. Leung, L. M. Sowa, H. H. Wang, J. M. Williams, and M.-H. Whangbo, *Solid State Commun.*, **57**, 735 (1986).

107) E. I. Zhilyaeva, R. N. Lyubovskaya, S. A. Torunova, S. V. Konovalikhin, O. A. Dyachenko, and P. B. Lyubovskii, *Synth. Met.*, **80**, 91 (1996).